

Discover the Possibilities

GC/MS Instrument Intelligence



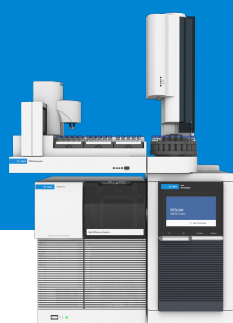


Overview

At ASMS 2023, Agilent continued to advance the state of the art in GC/MS. New tools, ranging from AI-enabled data processing to high-quality spectral libraries were demonstrated helping aid in real-world analytical challenges. Expanding the success of using the alternative carrier gas hydrogen, technical details were shared in environmental and food applications. Whether you attended the conference or not, stay up to date on the latest in GC/MS technology.



Agilent 5977C GC/MSD



Agilent 7000E GC/TQ



Agilent 7010C GC/TQ



Agilent 7250 GC/Q-TOF

Table of contents

Unit mass

AI Peak Integration for MassHunter Software Automates Manual Peak Integration During the Data Analysis Process in GC/SQ	4
Extraction and Analysis of Polycyclic Aromatic Hydrocarbons in Infant Formula	8
Helium to Hydrogen: Explosives and Pesticides and VOAs, Oh My! Successful Transition of GC/MS Analyses	14
Analysis of Nonylphenols and Phthalates from Food Contact Packaging using GC/MS/MS	18
Analysis of PAHs Using Hydrogen Carrier Gas and the Hydrogen-Optimized Source with GC/MS and GC/MS/MS in Challenging Soil Matrix	22
Automated Sample Preparation Using CTC PAL3 to Analyze >570 Pesticides in an Orange by the Combination of GC/MS/MS and LC/MS/MS Techniques	26
Achieving the MRLs with Hydrogen Carrier Gas: GC/MS/MS Analysis of 200 Pesticides in Produce	30

High resolution

Accurate Mass Library for PFAS Analysis in Environmental Samples Using High-Resolution GC/Q TOF	35
Differences in Metabolic Profiles of Individuals with Heart Failure Using High Resolution GC/Q-TOF	40

AI Peak Integration for MassHunter Software Automates Manual Peak Integration During the Data Analysis Process in GC/SQ

Authors: Thomas Bispham, Tamas King, Winnie Chau, and Ruoji Luo
Agilent Technologies, Inc.

Introduction

GC/MS data analysis is often manual, time consuming, and error-prone (Figure 1). Even though many automated integrators are available, a chemist may still need to manually correct integration peaks and baselines. A new quantitative analysis software automates peak integration during the data analysis process for analytical testing laboratories. A Machine Learning (ML) model is custom-trained through a user's standardized data analysis workflow, observing manual peak integration events. Machine Learning then replaces manual peak integration with adaptable artificial intelligence (AI)-assisted peak detection and integration with continuous learning.

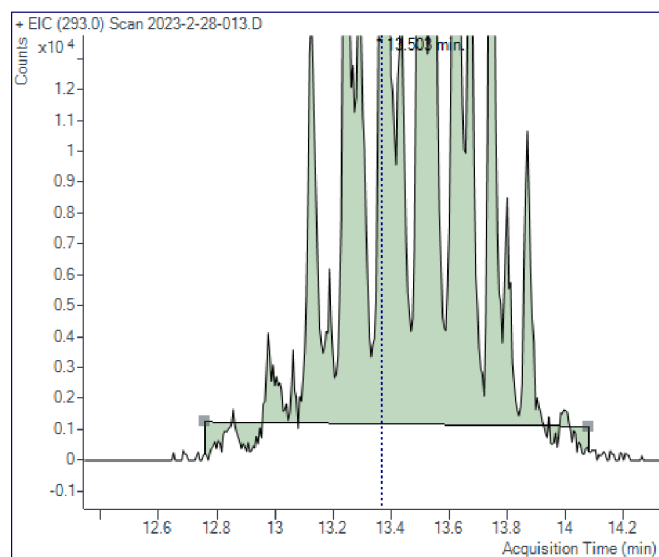


Figure 1. Manual integration often results in an inconsistent baseline, even for an expert chemist.

The novel peak integration software helps improve process automation, maximize sample throughput, and produce consistent and high-quality data while facilitating ease of adoption for laboratories.

Phthalate compounds are described as an "everywhere chemical" around the world¹, as they are heavily used in packaging and plastic materials.^{2,3} Manual integration of the compounds' high molecular weight proves difficult, even for an experienced analyst (Figure 2).

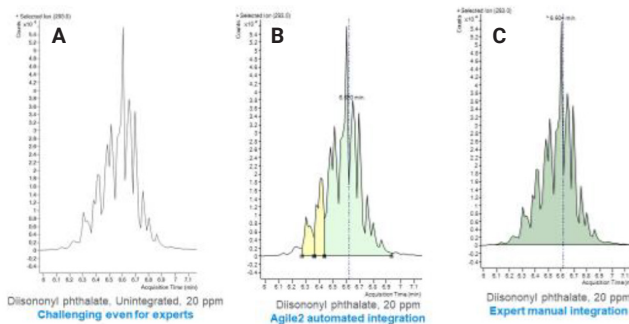


Figure 2. The challenge of integrating DINP and DIDP in phthalates with single quad GC/MS. (A) DINP in phthalates have GC/MS peaks that are partially coeluted. (B) DINP peak integrated by automated integrators; (C) DINP peak manually integrated by an expert chemist.

Experimental

Equipment and software

Agilent GC/MS (Single Quad) instruments were used to acquire samples. Agilent MassHunter (Version 10.2) software workstation was used for data acquisition and quantitation.

An add-on to MassHunter Quant was setup to communicate to the AI Peak Integration database, which was cloud-based. MassHunter Quant functions with a default parameterless integrator, Agile2, to analyze sample data. This was used as a basis for the Machine Learning model.

Modeling and data

A Machine Learning model was developed for the analysis of phthalate compounds in consumer products. Data from 1,247 real-world consumer samples were used to “train” a Machine Learning model in phthalate detection and quantitation. The sample set contained 800 to 1,000 positively-identified phthalate peaks.

Data info

Table 1. Data information.

Targeted Compounds	14 phthalates, 1 Internal Standard (ISTD)
Target Acquisition	SIM/Scan
Default Automatic Integrator	MassHunter Agile2 (parameterless)

Data analysis workflow

Samples and Method are combined into a MassHunter Batch. A chemist analyzes a batch in a consistent sequence, but manual integration is replaced by AI Peak Integration processing (Figure 3).

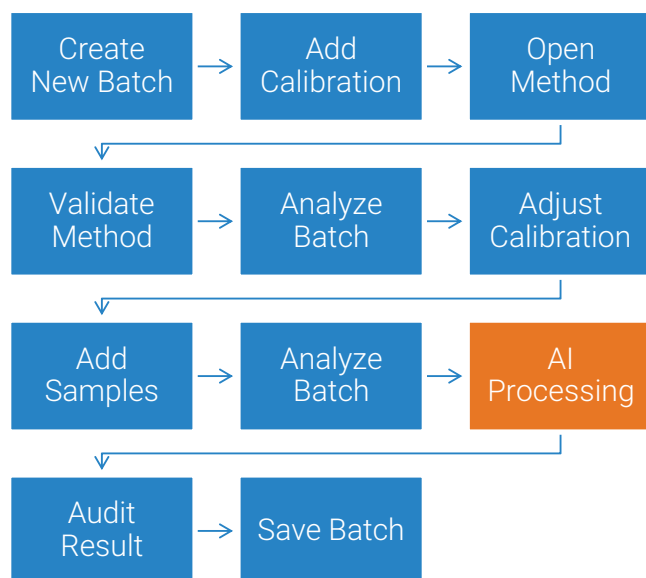


Figure 3. Batch processing workflow.

Results and discussion

Speed

Under ideal conditions with an expert analyst, reviewing data and performing manual integration requires an average of 60 to 120 seconds per chromatogram.

The AI Peak Integration solution outpaced manual integration after just a few positive samples. The minimum cloud processing time was approximately 30 seconds.

In preliminary testing, AI Peak Integration software performed peak integration on 100 samples in fewer than 25 minutes, where an expert chemist (under the ideal conditions) would take 2 hours to manually integrate peaks in the same batch, thus enabling at least a 4-times gain in productivity (Table 2).

Table 2. Manual versus AI-assisted integration estimates.

Phthalate Samples	Manual Chemist Integration Estimate (hrs)	AI Peak Integration Via Cloud Estimate (hrs)
25	0.44	0.10
50	0.88	0.19
100	1.76	0.39
1,000	17.6	3.9
10,000	176	39

In addition to speed, using a sufficiently-trained Machine Learning model improves integration quality when compared to the default integrator or manual integration.

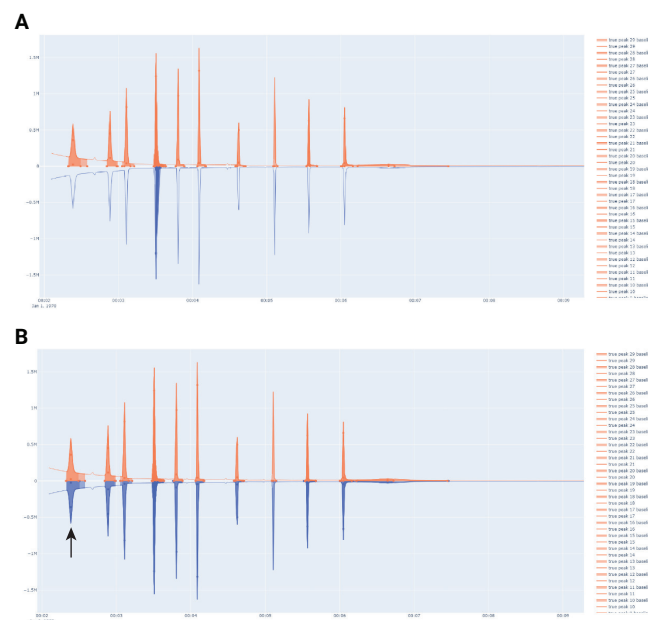


Figure 4. Comparison of a data-deficient Machine Learning model (A) and a sufficiently-trained model (B) with numerous positive samples. Solid orange peak is “truth”, based on chemist manual integration. Blue is predicted integration and identification of substance by AI Peak Integration.

Accuracy

Machine Learning model accuracy metrics improve with more sample submissions and more diverse data. Prediction of less-common phthalate compounds was shown to improve over time (Figure 5).

Data randomization was used to remove inherent bias when a ML model is trained on new or supplemental data.

When comparing a typical chemist's manual integration of peaks and baselines, the AI Peak Integration yielded greater precision, especially with uneven baselines (Figure 6).

Future

Machine Learning modelling holds promise for several applications in GC/MS. Extending the solution to other substances, such as regulated compounds in oil and gas, and additionally agriculture (pesticides) can benefit from reducing manual integration time of non-conventional peak shapes.

Environmental semivolatile organic compounds are candidates for future experimentation. Other substances, like short chain chlorinated paraffins (SCCPs, Figure 7) are also difficult to integrate.

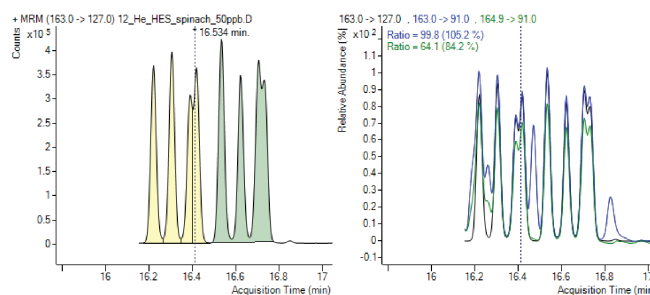


Figure 7. Peaks of short chain chlorinated paraffins could benefit from AI Peak Integration.

In addition to more analyte detection, other Machine Learning applications to chromatography might include calibration curve automation, and predictive maintenance.

Conclusion

Chemist time can be spent more valuably, due to:

- Reproducible results
- Universal consistency of analytical results
- Ease-of-use for expert and new lab analysts
- Reduced turnaround time
- Improved overall lab efficiency

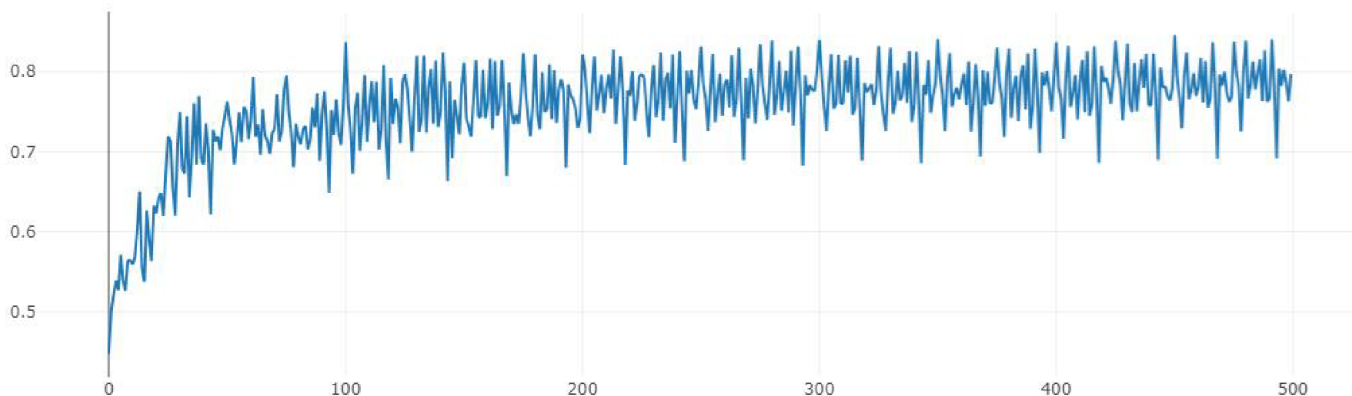


Figure 5. Critical Success Index (maximum of 1) of ML model measured on held-out data as training progresses.

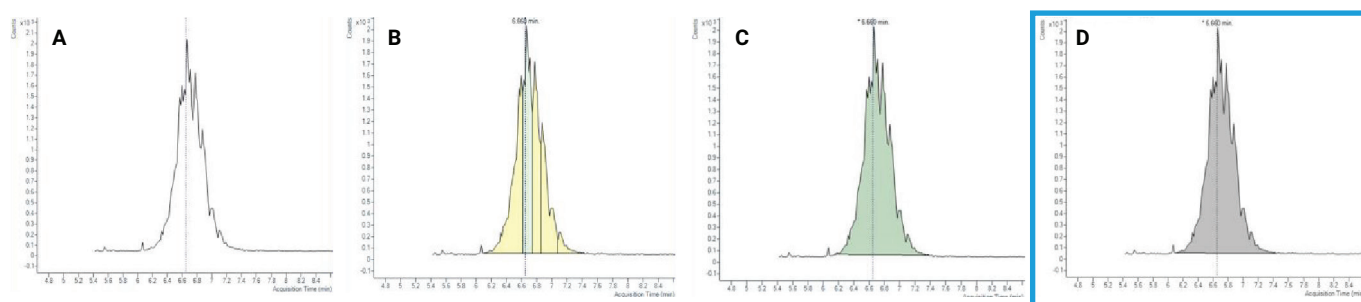


Figure 6. Comparison of peak detection of diisodecyl phthalate (DIDP). Left-to-right: (A) Not integrated, (B) integrated using Agilent MassHunter default parameter-less integrator (Agile2), (C) integrated manually by chemist, (D) integrated using AI Peak Integration for MassHunter.

References

1. Phthalates: The Everywhere Chemical
https://www.niehs.nih.gov/research/supported/assets/docs/j_q/phthalates_the_everywhere_chemical_handout_508.pdf
2. Phthalates and Cumulative Risk Assessment: The Tasks Ahead <https://pubmed.ncbi.nlm.nih.gov/25009926/>
3. Edwards *et al.* Phthalate and Novel Plasticizer Concentrations in Food Items from U.S. Fast Food Chains: a Preliminary Analysis, **2021**. doi: 10.1038/s41370-021-00392-8. <https://www.ncbi.nlm.nih.gov/pmc/articles/PMC9119856/>

Extraction and Analysis of Polycyclic Aromatic Hydrocarbons in Infant Formula

Authors: Jessica Westland, Limian Zhao, Anastasia Andrianova, Bruce Quimby, Tim Conjelko, and Lakshmi Krishan
Agilent Technologies, Inc.



Introduction

PAH exposure

One of the common ways for humans to encounter PAH exposure is through food consumption. Several countries have drafted legislation to establish tolerable limits for PAHs in foods, food products, and beverages, as well as to enforce monitoring strategies for the most relevant compounds.² Furthermore, regulatory agencies such as the World Health Organization (WHO) and the European Commission (EC) have launched regulations to decrease the concentration of PAHs in food, especially through strategies to control the processes that induce their formation.²

There is particular concern about the levels of PAHs in infant formula. The EC defines infants as "children under the age of 12 months," and infant formula as "food used by infants during the first months of life and satisfying by

themselves the nutritional requirements of such infants until the introduction of appropriate complementary feeding".³ The current European legislation provides specific PAH parameters for processed cereal-based food and baby food for infants and young children; infant formulae; and follow-on formulae.⁴ According to Commission Regulation (EU) number 835/2011, the content of benzo[a]pyrene (BaP) and PAH4 (the sum of BaP, benz[a]anthracene (BaA), benzo[b]fluoranthene (BbF), and chrysene (Chr)) in processed cereal-based food and baby food for infants and young children should not exceed 1 µg/kg.

H₂ carrier

GC/MS is the most commonly used technique for analysis of PAHs allowing for trace analysis of PAHs in foods with selectivity and sensitivity. With the increased global helium (He) crisis in the market, laboratories are looking for a more sustainable alternative to helium and exploring the option of H₂ carrier gas. The economic benefits of H₂ carrier gas for GC are widely known but resulting hydrogenation and dechlorination reactions in the MS source may occur, and thus make the application of H₂ for GC/MS challenging. The Agilent HydroInert source is a newly designed extractor source for GC/MSD that addresses these issues and improves performance with H₂ carrier gas in GC/MS.¹

Sample preparation

Agilent Captiva EMR–Lipid pass-through cleanup

Low regulatory limits and food matrices add layers of complexity to the analysis of PAHs. Several factors can affect the quantification of PAHs, such as solubility, temperature, ionic strength, interactions with the matrix of origin, and so on. As a result, an extensive, multistage sample preparation method is necessary.

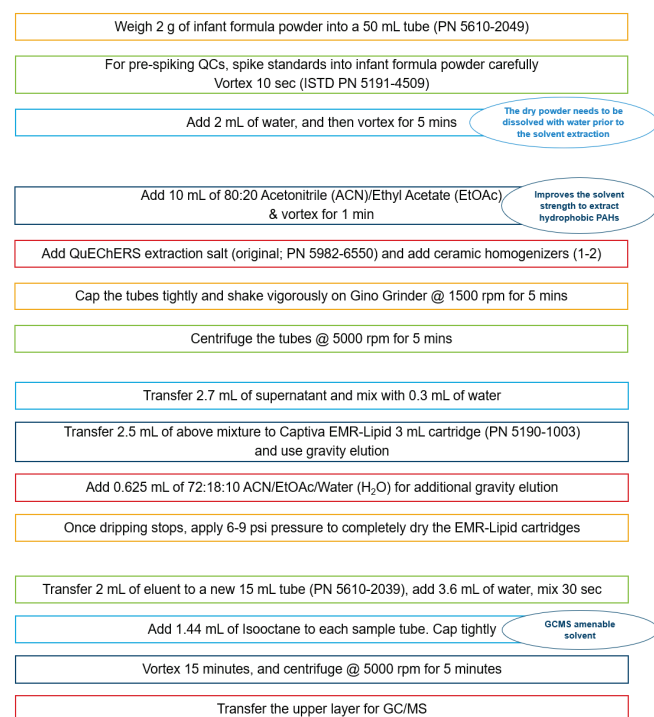


Figure 1. Workflow diagram.

- Infant formula is a relatively fatty food matrix, containing 5 to 20% fat. It is required to dissolve the dry powder first to achieve the efficient solvent extraction.
- The water addition to dissolve the infant formula powder was investigated by comparing the typical water volume of 10 mL to the much smaller volume of 2 mL. Figure 1 shows the targets recovery comparison using the two different water addition volume. The results clearly demonstrated that the smaller water volume (2 mL) for powder dissolving played an important role for heavy PAHs recoveries. This is because the larger water volume (10 mL) can result in the reduced solubility of more hydrophobic

PAHs and cause the loss of these targets during extraction. As a result, 2 g of infant formula was dissolved into 2 mL of water for the following solvent extraction.

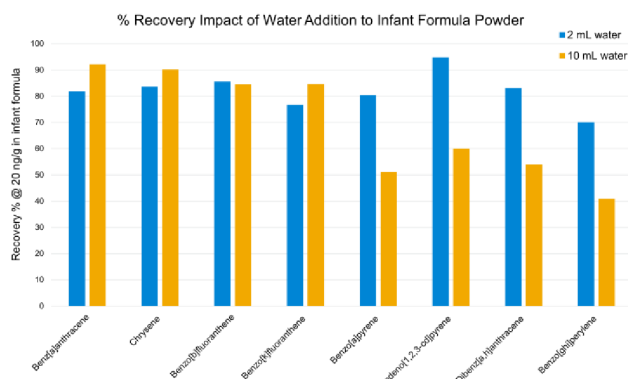


Figure 2. Target recovery comparison using different water addition volumes.

- After solvent extraction from the infant formula matrix, a cleanup/purification step is essential to isolate the analytes of interest and to remove potential interferences, especially fatty co-extractives such as triglycerides and fatty acids, where Captiva EMR–Lipid can provide an efficient matrix cleanup.²
- The use of 20:80 EtOAc:ACN for the extraction provides enough strength to extract hydrophobic PAHs from fatty matrices.
- The Captiva EMR–Lipid pass-through cleanup has gained considerable attention since its introduction. The EMR–Lipid sorbent selectively interacts with the unbranched hydrocarbon chains of lipids, leaving "bulky" target analytes in solution for subsequent analysis.
- The additional elution on Captiva EMR–Lipid assures the complete elution of targets from Captiva EMR–Lipid cartridges during pass-through cleanup.
- The isooctane back extraction after cleanup makes it easier to switch from the extraction solvent to a more GC-amenable solvent and provides partial sample concentrating.
- The entire sample preparation procedure introduces a 5× dilution of the infant formula powder sample.

Infant formula matrix chromatograms

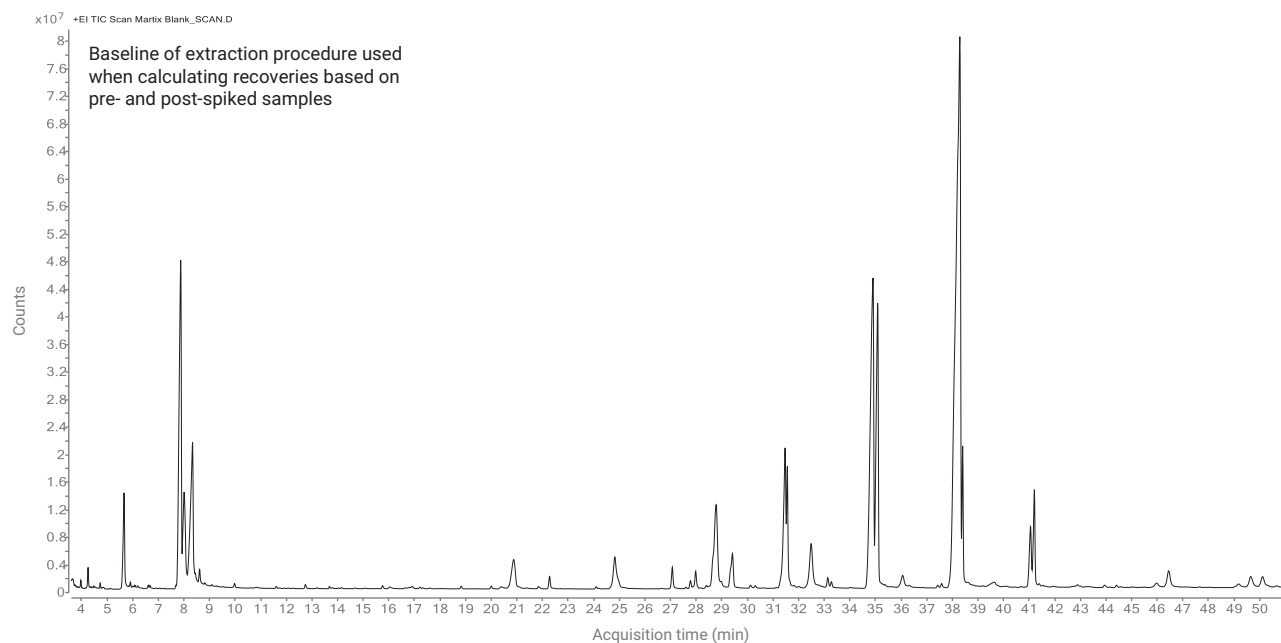


Figure 3. A GC/MS total ion chromatogram (TIC) scan of the infant formula.

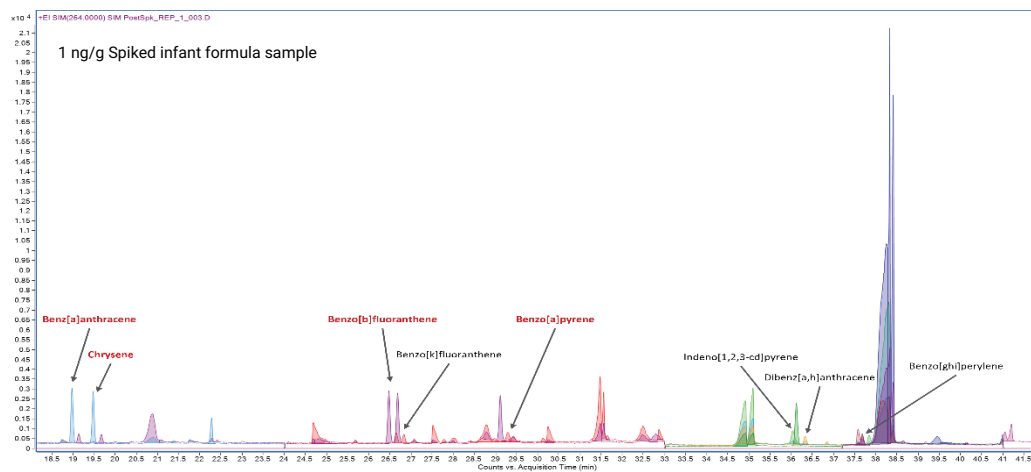


Figure 4. A GC/MS SIM chromatogram of PAHs in post-spiked infant formula.

Agilent Hydrolnert Source

Instrument

GC/MS is the preferable mode of detection as it confirms the identity of the analyte with high selectivity and for using stable isotope labeled PAHs as internal standards, thereby reducing analytical errors.¹ Tables 1 and 2 provide information on the instrumentation and consumables, as well as the parameters, respectively.



Agilent 8890/5977C GC/MS.

Table 1. GC and MSD instrumentation and consumables.

Part	Description
GC	Agilent 8890 GC system
MS	Agilent 5977C Inert Plus GC/MSD
Source	Agilent Hydrolnert source with 9 mm Hydrolnert extraction lens
Syringe	Agilent Blue Line autosampler syringe, 10 µL, PTFE tip plunger (p/n G4513 80203)
Column	Agilent J&W DB EUPAH GC column, 20 m × 0.18 mm, 0.14 µm, 7-inch cage (p/n 121-9627)
Inlet Liner	Agilent inlet liner, Ultra Inert, split, low pressure drop, glass wool (p/n 5190-2295)

Table 2. GC and MSD instrument conditions.

Parameter	Value
Injection Volume (L1)	2 µL
Injection Type	Two-layer sandwich (L1, L2)
L1 Air Gap	0.2 µL
L2 Volume	0.5 µL (used for ISTD sandwich injection)
L2 Air Gap	0.2 µL
Inlet Temperature	320 °C
Inlet Mode	Pulsed splitless
Septum Purge Flow	3 mL/min
Septum Purge Flow Mode	Switched
Injection Pulse Pressure	40 psi until 0.75 min
Purge Flow to Split Vent	50 mL/min at 0.7 min
Column Temperature Program	60 °C (1 min hold); 60 °C/min to 180 °C (hold 0 min); 3 °C/min to 335 °C (hold 15 min)
Carrier Gas and Flow Rate	H ₂ , 0.9 mL/min constant flow
Transfer Line Temperature	320 °C
Ion Source Temperature	320 °C
Quadrupole Temperature	150 °C
Data Acquisition	Selective ion monitoring (SIM)
Tune	etune.u
Gain Factor	5



Agilent Hydrolnert source .

Due to recent pressures on the helium (He) supply, required organizations have had to actively investigate the use of hydrogen (H₂) carrier gas. However, most GC/MS analyses have reduced sensitivity and hydrogenation or dechlorination in the source. The PAHs extraction from infant formula was performed using H₂ and the Agilent Hydrolnert source on the Agilent 8890/5977C GC/MS.

- Allows for the use of hydrogen carrier gas with better supply and reduced cost
- Faster, shorter separations
- Reduces loss of sensitivity and spectral anomalies
- Reduced source cleanings and maintenance

Results and discussion

Method recovery and reproducibility

Target analyte recoveries for eight PAHs were calculated based on the direct peak-area comparison of the prespiked and postspiked infant formula samples, and the results are shown in Figure 5. The four critical PAH compounds—BaP, BaA, BbF, and Chr—are circled in red. Three levels of spiked samples were used for method recovery and reproducibility validation, which included 1, 10, and 50 ng/g in infant formula with six replicates at each level.

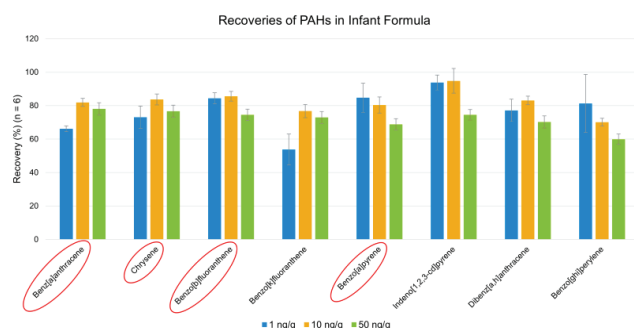


Figure 5. Method recoveries and reproducibility for targeted PAHs in infant formula.

Table 3. Analysis data for target PAHs.

Compound	RT (min)	Linearity	Quantifier Ion (m/z)	Qualifier Ion 1 (m/z)	Qualifier Ion 2 (m/z)
Benzo[a]anthracene-d12	19.00	0.999	240.1	236.1	
Benz[a]anthracene (BaA)	19.15		228	226	229
Chrysene-d12	19.50	0.997	240	236	
Chrysene (Chr)	19.69		228.1	226.1	229
Benzo[b]fluoranthene-d12	26.50	0.998	264	260	
Benzo[b]fluoranthene (BaF)	26.67		252	250	253
Benzo[k]fluoranthene-d12	26.70	0.994	264.1	260.1	
Benzo[k]fluoranthene	26.85		252	250	253
Benzo[a]pyrene-d12	29.14	0.995	264.1	260.1	
Benzo[a]pyrene (BaP)	29.31		252.1	250.1	248
Indeno[1,2,3-cd]pyrene-d12	35.91	0.998	288	284	
Indeno[1,2,3-cd]pyrene	36.05		276	274	277
Dibenzo[a,h]anthracene-d14	36.14	0.998	292	288	
Dibenz[a,h]anthracene	36.35		278.1	276.1	279.1
Benzo[ghi]perylene-d12	37.71	0.997	288	287	
Benzo[ghi]perylene	37.86		276.1	274.1	277
Dibenzo[a,i]pyrene-d14	46.45		316	317	

The results confirmed that the method delivered acceptable >60% recoveries (60 to 95%) with <20% RSD, except for benzo[k]fluoranthene at 1 ng/g level (54% recovery), and benzo[ghi]perylene (34.6% RSD). The two outliers are mostly due to the low sensitivity of the instrument detection method and greater matrix impact at the 1 ng/g level. The instrument method sensitivity and matrix impact to low-level spiked samples also resulted in higher RSDs at the 1 ng/g level.

Analytical system

For quantitation of PAHs in infant formula, a matrix-matched calibration was used with seven calibration levels from 0.1 to 20 ppb in vial (0.5 to 100 µg/kg in infant formula). Target analyte retention times (RTs) and linearity values are displayed in Figure 6 and Table 3.

Acquiring a quantitation level below 1 µg/kg for BaP and PAH4 allows accurate quantitation for the Commission Regulation (EU) number 835/2011.

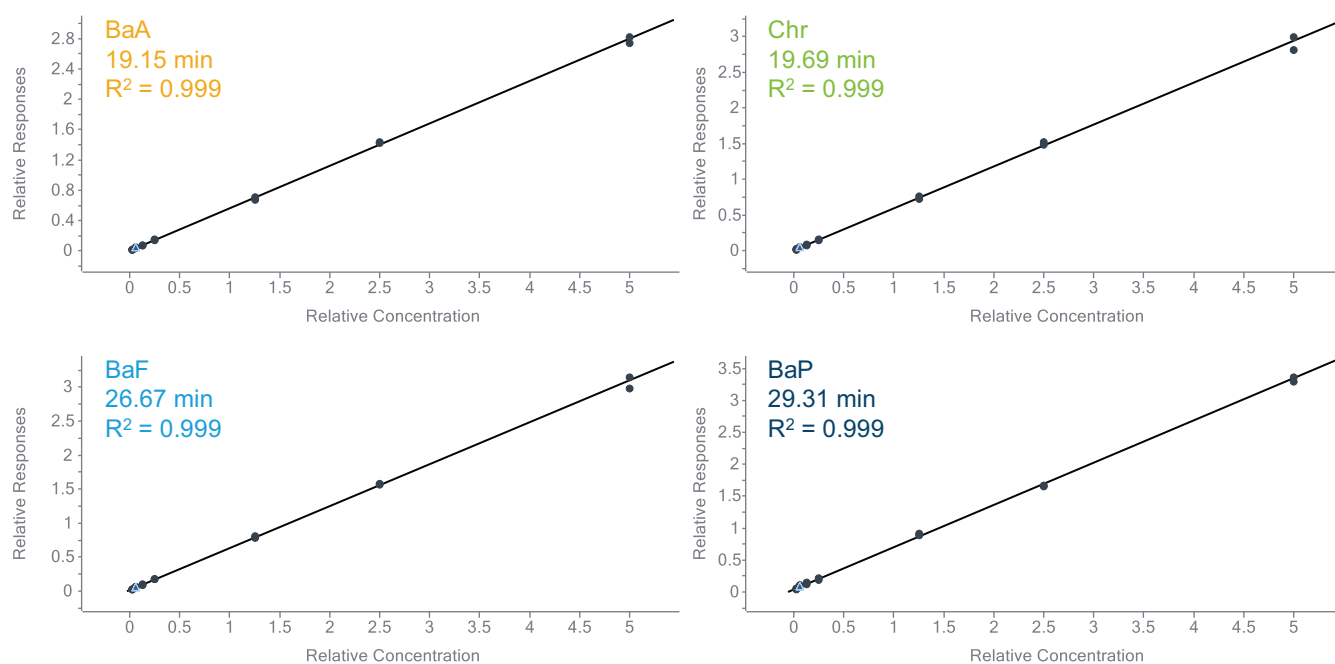


Figure 6. Matrix-matched calibration for PAH4 seven calibration over 0.1 to 20 ppb in vial (0.5 to 100 µg/kg in infant formula).

Conclusion

- An Agilent Captiva EMR–Lipid pass-through cleanup for PAH analysis in infant formula and the use of the Agilent Hydrolnert source with H₂ carrier gas on the Agilent 8890 GC and 5977C GC/MSD system can be used for the determination of PAHs at low concentrations.
- The method delivered acceptable recovery, reproducibility, and quantitation results that meet the EU regulation for PAH analysis in food.

References

1. Agilent Inert Plus GC/MS System with Hydrolnert Source, *Agilent Technologies technical overview*, publication number 5994-4889EN, **2022**.
2. Sampaio, G. R. *et al.* Polycyclic Aromatic Hydrocarbons in Foods: Biological Effects, Legislation, Occurrence, Analytical Methods, and Strategies to Reduce Their Formation. *Int. J. Mol. Sci.* **2021**, 22(11), 6010. DOI: <https://doi.org/10.3390/ijms22116010>
3. European Commission, Food for Infants and Young Children. https://food.ec.europa.eu/safety/labelling-and-nutrition/specific-groups/food-infants-and-young-children_en (accessed 2022-11-14).
4. The European Commission, Commission Regulation (EU) No 835/2011 of 19 August **2011** Amending Regulation (EC) No 1881/2006 as Regards Maximum Levels for Polycyclic Aromatic Hydrocarbons in Foodstuffs. *Official Journal of the European Union. L* 215/4, rev 08.2011.
5. Zhao, L.; Wong, D. Determination of 19 Polycyclic Aromatic Hydrocarbon Compounds in Salmon and Beef, *Agilent Technologies application note*, publication number 5994-0553EN, **2020**.
6. Akinpelu, A. A. *et al.* Polycyclic Aromatic Hydrocarbons Extraction and Removal from Wastewater by Carbon Nanotubes: A Review of the Current Technologies, Challenges and Prospects. *Process Saf. Environ. Prot.* **2019**, 122(10), 68–82.
7. Purcaro, G.; Barp, L.; Moret, S. Determination of Hydrocarbon Contamination in Foods. A review. *Anal. Methods* **2016**, 8(29), 5755–5772.

Helium to Hydrogen: Explosives and Pesticides and VOAs, Oh My! Successful Transition of GC/MS Analyses

Authors: Eric Fausett, Anastasia Andrianova, Bruce Quimby, Angela Smith Henry, Kirk Lokits, Limian Zhao, Jessica Westland, Samuel Haddad, Jonathan Osborn, and Aaron Boice
Agilent Technologies, Inc.

Introduction

Helium is the best and most used carrier gas in GC/MS. Hydrogen is the second-best alternative to helium. It provides several advantages, including faster analysis times and smaller environmental impact. However, hydrogen is a reactive gas. Hence, every analyte in every method needs to be validated with hydrogen.

This work provides guidance on the GC/MS conditions for the effective transition from helium to hydrogen carrier gas for a variety of applications.

Experimental

HydroInert Source

The HydroInert source is an EI source optimized for use with hydrogen carrier gas. Due to its inert nature, it minimizes undesirable in-source chemical reactions between the analytes and hydrogen. This results in improved library match scores (LMS) versus helium-based libraries and allows for the use of the same target ions in GC/MS and MRM transitions in GC/MS/MS. This makes the transition of methods from helium to hydrogen much easier.

Considerations for GC/MS method conversion

The following should be considered when converting from helium to hydrogen.

- Review the document “The EI GC/MS Instrument Helium to Hydrogen Carrier Gas Conversion Guide”¹ for detailed instructions for method conversion from He to H₂ carrier. This covers all aspects, including H₂ safety, that should be considered.
- When targeting fragile analytes like pesticides or explosives, use a temperature programmable inlet like the MMI to minimize possible hydrogenation reactions.
- Use the Agilent Method Translation calculator¹ to pick a column and parameters to obtain the same elution order as with the helium method. Since most helium methods use a 30 m × 0.25 mm id column, the 20 m × 0.18 mm version is a great place to start.
- The increased resolution afforded by hydrogen may allow the development of a faster method.
- For the reasons mentioned above, use the HydroInert source.

Results and discussion

Pesticides

Figure 1 compares the chromatograms for 203 pesticides in a spinach QuEChERS extract with He and with the optimized H₂ method. Using Method Translation, the elution order and retention times are the same, greatly simplifying conversion. Note the increased resolution with H₂. This can be further exploited with Method Translation to decrease the run time from 20 minutes to 10 minutes.² The optimized H₂ method uses the MMI inlet with a temperature programmed solvent vent injection of 2 µL. A 2 mm dimpled liner and HP-5MS UI 20 m × 20 m (0.18 mm × 0.18 µm) column set in backflush configuration are also used. With the H₂ optimized method, over 90% of the 203 targets could be quantitated at or below 10 ppb (mg/kg) in spinach extract, which is the default MRL.²

Volatile organic compounds in drinking water with headspace-GC/MS

H₂ carrier allowed the separation of 80 volatile organic compounds (VOCs) in 7 minutes. The method used a DB-624 20 m (0.18 mm × 1 µm) and a pulsed split injection of 20:1. Complete method details and results are provided in reference 3. Scan mode demonstrated excellent spectral matching against the NIST20 library (average LMS 94), and excellent calibration linearity with an average range of 0.16 to 25 µg/L. In SIM mode, the average range was 0.07 to 25 µg/L, and the average MDL for the 80 compounds was 0.026 µg/L. Figure 2 shows the chromatogram and highlights the excellent results for nitrobenzene, which is often a problem with H₂ carrier if the HydroInert source is not used.

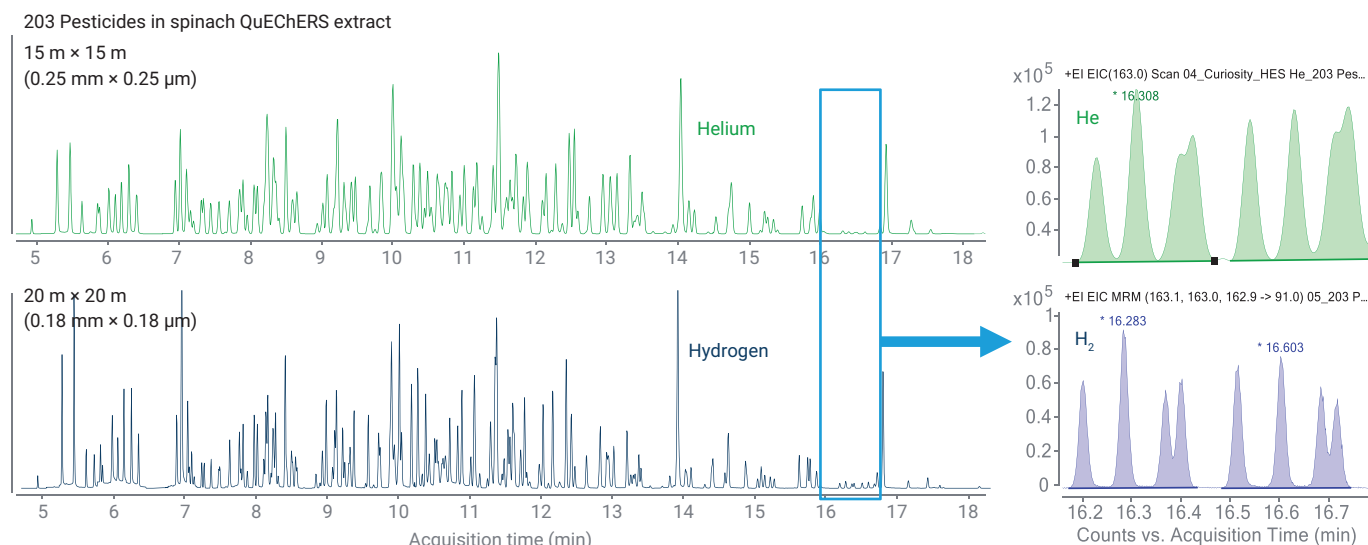


Figure 1. (A) Pesticide method with He carrier. (B) Method converted to H₂ carrier using 0.18 mm id column set.

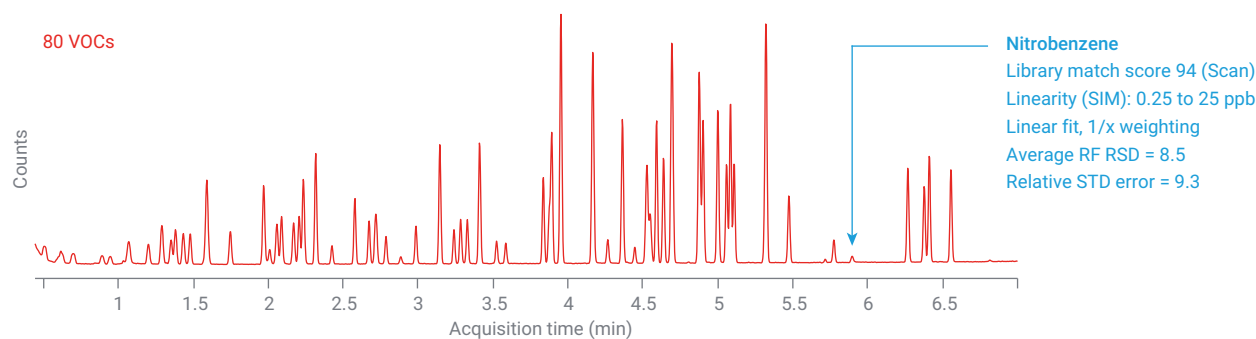


Figure 2. VOCs in water analyzed by headspace/GC/MS.

Semivolatile organic compounds (SVOCs) with EPA 8270E

Figure 3 shows the analysis of 120 target analytes and surrogates using H₂ carrier gas, the HydroInert source and the 7000E GC/TQ. The use of H₂ carrier and the 0.18 mm id column provided excellent resolution and a run time of only 10.5 minutes. A 20:1 split injection was used and the MMI inlet was programmed from 250 °C (hold 0.3 minutes) at 200 °C/min to 350 °C. A calibration range of 0.02 to 100 µg/mL was obtained for 82 compounds and 0.1 to 100 µg/mL for 106 compounds. Note the excellent peak shape and resolution in Figure 3. Full details are available in reference 4. Excellent results were also obtained using the 5977C single quadrupole GC/MSD with H₂ carrier and the HydroInert source. This is detailed in reference 5.

Polynuclear aromatic hydrocarbons (PAHs)

PAHs are durable compounds that tend to tail with He carrier gas. With H₂ carrier and the HydroInert source, the peak shape and resolution are significantly improved, as shown in Figure 4. With 5977C GC/MSD, the MDL and linearity are comparable to or better than those with He. Also, the ISTD response was stable across four orders of calibration. Excellent linearity was observed over the range of <1 to 1,000 µg/L with an average RSE = 9.5. The average MDL was about 0.1 µg/L. Due in part to the cleaning action of H₂, response stability was shown over 100 injections of a challenging soil extract with GC/MSD. Full details are available in reference 6. Excellent results were also obtained using the 7000E GC/TQ with H₂ carrier and the HydroInert source. That system was configured with backflushing and response stability was shown over 500 injections with the challenging soil extract. This is detailed in reference 7.

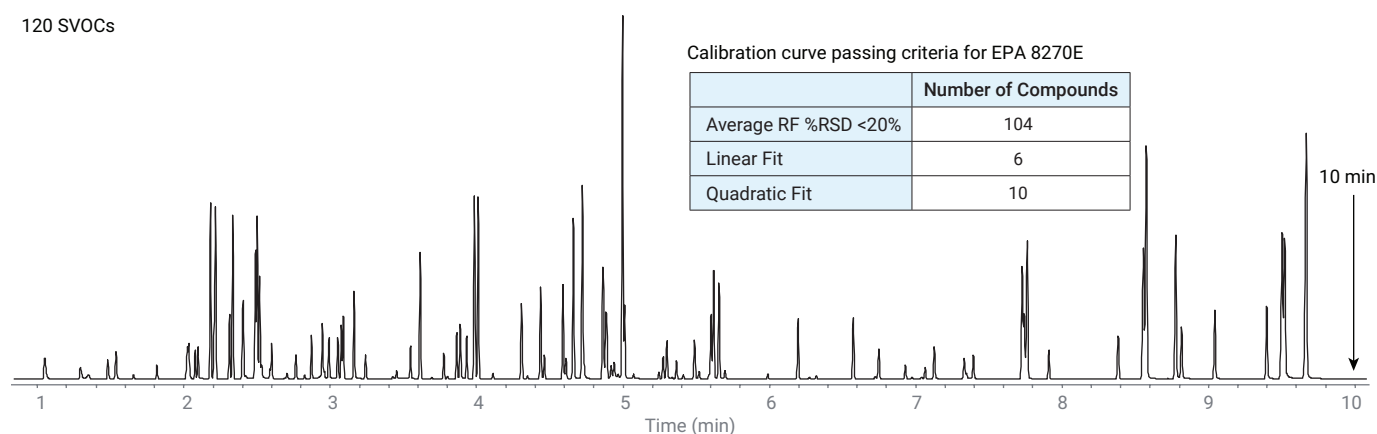


Figure 3. TIC of 120 SVOCs in method converted to H₂ carrier using an Agilent DB-5ms UI, 20 m × 0.18 mm id, 0.18 µm column.

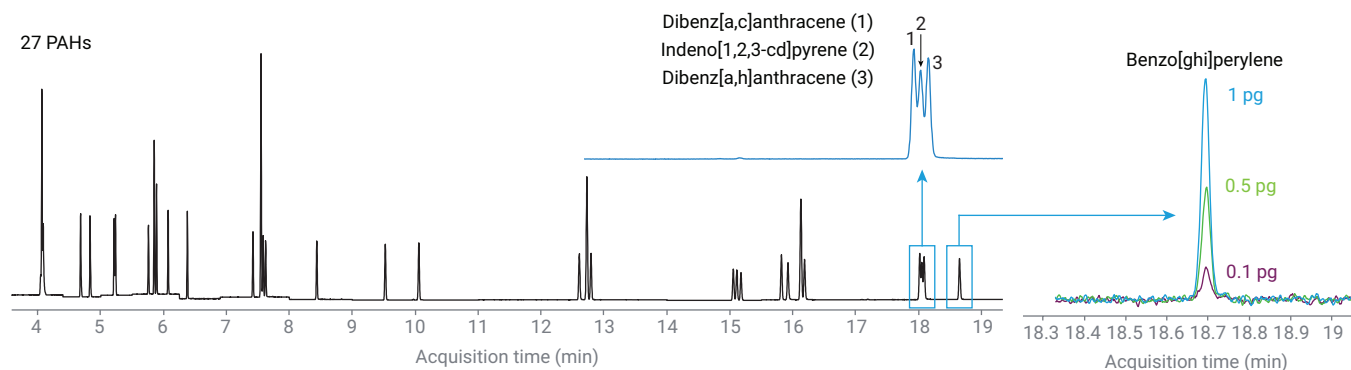


Figure 4. SIM TIC of 27 PAHs in method converted to H₂ carrier using an Agilent DB-EUPAH, 20 m × 0.18 mm id, 0.14 µm column.

Explosives

Nitro compounds used in explosives are highly prone to hydrogenation, leading to poor library match scores

(LMS) with H₂ carrier and traditional EI sources. A group of nitroaromatics commonly encountered in explosives were analyzed using a 50:1 temperature ramped split injection, a 20 m × 180 μm, 0.18 μm DB-5ms UI column, and the HydroInert source with H₂ carrier gas in the 5977C GC/MSD. As shown in Figure 5, excellent LMS values were obtained, indicating minimal hydrogenation.

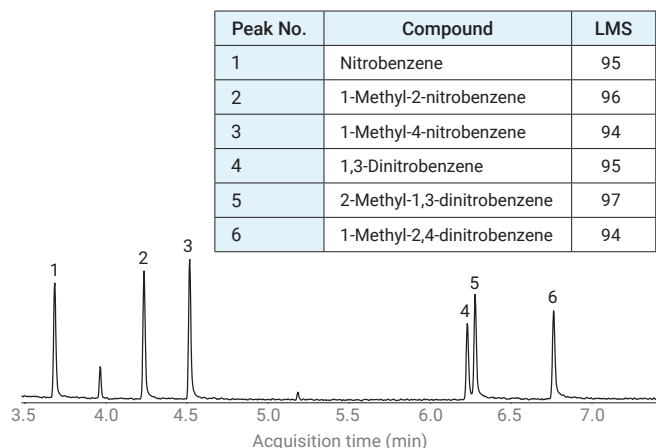


Figure 5. TIC of nitroaromatic compounds.

Conclusion

If He is available at an acceptable price, it is the preferred carrier for GC/MS and should be used. However, as shown in this overview of several converted methods, H₂ can be used if appropriate adjustments are made to accommodate its use.

References

1. Agilent EI GC/MS Instrument Helium to Hydrogen Carrier Gas Conversion. *Agilent Technologies user guide*, publication number 5994-2312EN. **2022**.
2. Achieving the MRLs with Hydrogen Carrier Gas: GC/MS/MS Analysis of 200 Pesticides in Produce. *ASMS Poster MP 225 ASMS* **2023**.
3. Volatile Organic Compounds Analysis in Drinking Water with Headspace GC/MSD Using Hydrogen Carrier Gas and HydroInert Source, *Agilent Technologies application note*, publication number 5994-4963EN, **2022**.
4. Analysis of Semivolatile Organic Compounds with Hydrogen Carrier Gas and HydroInert Source by Gas Chromatography/Triple Quadrupole Mass Spectrometry (GC/MS/MS), *Agilent Technologies application note*, publication number 5994-4891EN, **2022**.
5. Analysis of Semivolatile Organic Compounds Using Hydrogen Carrier Gas and the Agilent HydroInert Source by Gas Chromatography/Mass Spectrometry, *Agilent Technologies application note*, publication number 5994-4890EN, **2022**.
6. Analysis of PAHs Using GC/MS with Hydrogen Carrier Gas and the Agilent HydroInert Source, *Agilent Technologies application note*, publication number 5994-5711EN, **2022**.
7. GC/MS/MS Analysis of PAHs with Hydrogen Carrier Gas, *Agilent Technologies application note*, publication number 5994-5776EN, **2022**.

Analysis of Nonylphenols and Phthalates from Food Contact Packaging using GC/MS/MS

Authors: Matthew Curtis; David A. Weil
Agilent Technologies, Santa Clara, CA

Introduction

The production of antioxidants and surfactants used for the manufacturing of plastics and rubber use alkylphenol polyethoxylates which degrade into a group of alkylphenols called nonylphenols. In addition to the nonylphenols, phthalates can migrate from the plastic packaging to the material it is in contact with.¹ Nonylphenols are not fully degraded from sewer treatment procedures which leads to accumulation in river and ground water that can be absorbed by plants and animals. The concentration and composition of the nonylphenols and phthalates depend on the individual production of the plastic or rubber. Many of the previous application notes and publications utilized the seminonpolar capillary GC column, but that does not separate the isomers of the phthalates and nonylphenols required for confident peak integrations. The MRM transitions are not unique for the isomers, which means chromatographic separation is needed. In this work, the GC column and separation were optimized to obtain the ultimate detection limit for these analytes using a high efficiency ion source and MRM.

Experimental

Several different column phases were tested to determine which provided the best separation of a technical mixture of nonylphenols, phthalates and teraphthalates. These columns were all 30 m × 0.25 mm, 0.25 µm dimensions: HP-5ms UI, DB-17ms, DB-35, and VF-Xms. These all have different amounts of phenyl in the backbone as well as some proprietary chemistries to help with unique separations.



Figure 1. Agilent 8890 and 7010C GC/TQ.

The nonylphenol calibration standard, phthalate mix, and the terephthalate solutions were purchased from AccuStandard (New Haven, CT). These were mixed together and injected on each column, using a similar oven program, to evaluate the separation and select the best column.

Table 1. GC/TQ acquisition parameters.

GC and MS Conditions	GC/TQ (7010C)
GC	Agilent 8890
Column	Agilent DB-35ms UI, 20 m × 0.18 mm, 0.18 µm
Inlet	MMI, 4-mm UI Fritted Low
Injection Volume	1 µL
Injection Mode	Cold Pulsed-Splitless; 40 psi for 1.1 min
Inlet Temperature	50 °C; hold 0.05 min
Air Cooled	600 °C/min to 280 °C
Oven Temperature Program	70 °C for 1 min; 30 °C/min to 200 °C, 15 °C/min to 235 °C; hold 0.5 min, 5 °C/min to 245 °C, 45 °C/min to 300 °C; hold 2.73 min
Carrier Gas	Helium
Column Flow	0.9 mL/min
Transfer Line Temperature	300 °C
Quadrupole Temperature	150 °C
Source Temperature	280 °C
Collision Cell Flows	4 mL/min He; 1.5 mL/min N ₂
Acquisition Mode	dMRM

For the sample extracts, 100 mg of four different plastic food packaging materials (plastic wrap, plastic sandwich bag, to-go #5 polypropylene and to-go #6 polystyrene) were placed in a vial with a 10 mL of 4:1 hexane:ethyl acetate solution. The vials were sonicated at 60 °C for 30 minutes. The extraction was dried under a low flow of N₂ to dryness. 1 mL of fresh solvent was added and the sample was decanted into a clean glass vial and centrifuged for 10 minutes at 10,000 rpm.

Results and discussion

GC optimization

It does not matter how sensitive or unique the MS you are using is if the analytes cannot make it through the inlet and column. The UI low fritted liner was selected to help volatilize the high boiling phthalates, and the increased surface area allows for cold injections to minimize analyte degradation. Figure 2 illustrates the benefit of a cold injection with respect to a reduced shoulder and better response.

Optimal chromatographic separation was more difficult due to the additional phthalates and terephthalates added to the nonylphenol technical mixture. All of the analytes include a central phenyl group but the functional group lengths, compositions and positions dictated the retention on the different phases of columns. A small set of the phenyl backbone class columns were selected to identify the version the reduced coelutions. In order of increasing polarity; HP-5ms, VF-Xms, DB-35ms, and the DB-17ms were all tested for this analysis. The phthalate and terephthalate pairs were the first set of analytes that were reviewed to determine the best phase (Figure 3).

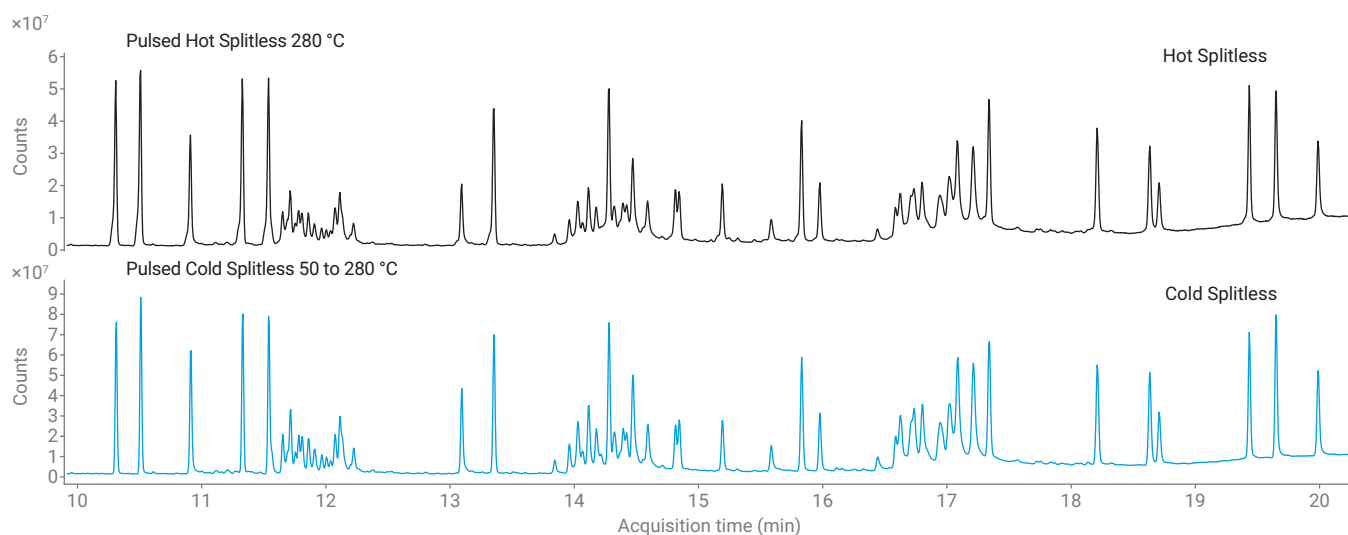


Figure 2. Comparison of the different inlet modes to reduce peak shoulders for the early eluters and increase signal intensity. The black chromatogram was created with an isothermal hot pulsed splitless injection while the blue was from a cold pulsed splitless injection that ramped to 280 °C.

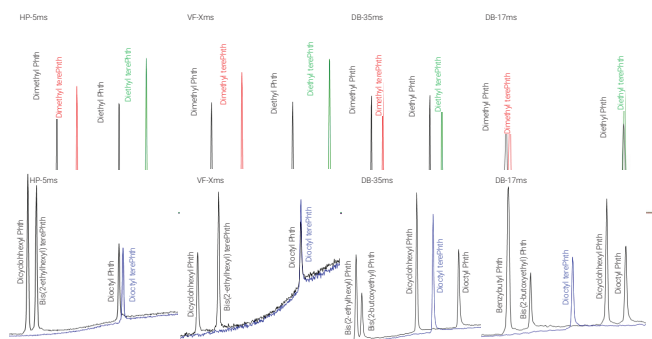


Figure 3. Due to the complexity of the separations, the HP-5ms and DB-35ms were the only columns to baseline separate each of the phthalate isomers. These could not be separated using the MS.

The next critical separation is between the phthalates, and nonylphenols, nonylphenol monoethoxylates and nonylphenol diethoxylates. The only major coelution occurred within the nonylphenol monoethoxylates and a few phthalates. These compounds could be separated using unique ions for each compound at the specified retention time. The HP-5ms and VF-5ms columns showed overlap of the monoethoxylates and both dibutyl and bis(2-methoxyethyl) phthalate. Only Dibutyl phthalate eluted within the monoethoxylates on the DB-35ms and the DB-17 ms (Figure 4). The DB-35ms phase was selected as the best phase to separate the analytes; for the optimized method a 20 m × 0.18 mm, 0.18 μm DB-35ms was optimized for minimal runtime (Figure 5).

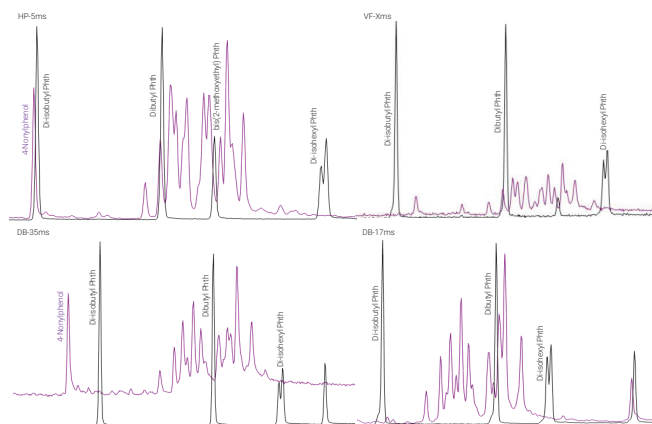


Figure 4. Overlaid chromatogram for the four columns tested to illustrate the need for a higher polarity column to help separate the phthalates and the nonylphenol monoethoxylate isomers. 4-Nonylphenol and di-isobutyl phthalate almost coelute on the HP-5ms column.

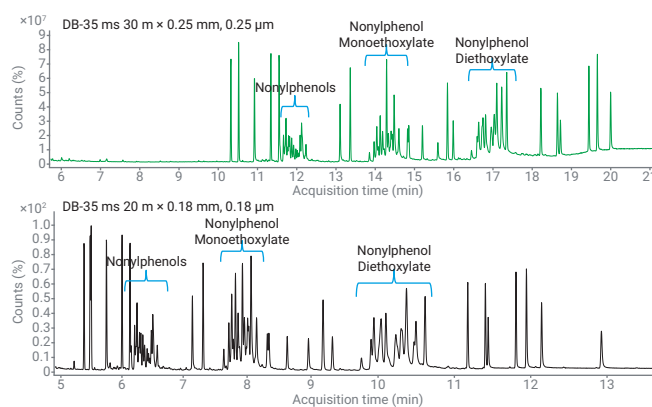


Figure 5. Overlaid chromatogram for the four columns tested to illustrate the need for a higher polarity column to help separate the phthalates and the nonylphenol monoethoxylate isomers. 4-Nonylphenol and di-isobutyl phthalate almost coelute on the HP-5ms column.

MS/MS Optimization

The complexity and number of components in this analysis creates a challenge for the method creation. Manually injecting, analyzing the results, and creating a method for the next injection will take a significant amount of time for each MRM transition. MRM Optimizer was used to automate this process after the GC method was completed. The full scan data from the optimized method is loaded into the software, deconvolution extracts single component spectra which are analyzed and the precursor ions are selected automatically. MRM Optimizer will create the product ion method, run the sample, analyze the results to find the optimal product ions, and finally optimize the collision energy for each transition (Figure 6). Figure 7 provides the chromatograms for the extracted samples.

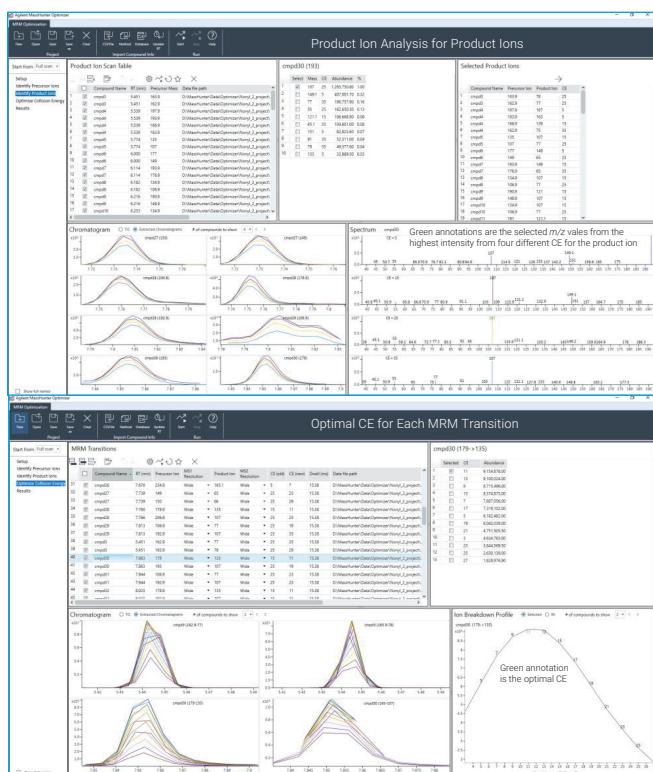


Figure 6. The two main steps for MRM Optimizer to create the MRM transition for the analytes.

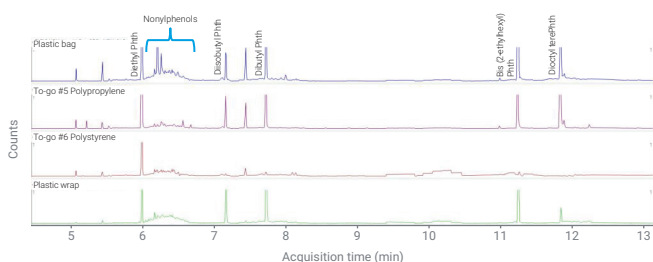


Figure 7. Stacked chromatograms for the extracted plastic packaging material. The wrap and bag both extracted the most nonylphenols.

Phthalates, terephthalates, and the nonylphenol standards were all detected at the 1 fg/ μ L concentration (Figure 8). Diethyl phthalate is not included due to this compound being found in multiple components from the sample prep and introduction. The glassware and glass micropipetter were cleaned with multiple solvents prior to the dilutions.

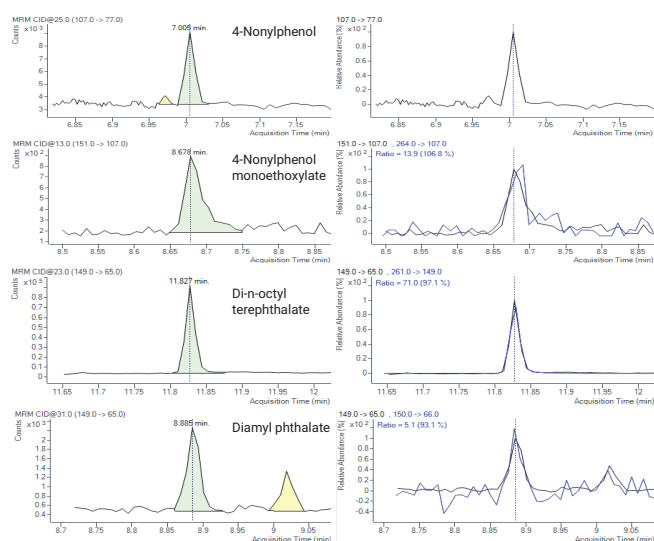


Figure 8. MRM transitions for the phthalate, terephthalate, 4-nonylphenol, and 4-nonylphenol monoethoxylate at 1 fg/ μ L.

Conclusion

- The DB-35ms column and a cold pulsed splitless injection provided the best combination for separation, peak shape and intensity for this analysis.
- The phthalates and terephthalates were detected at the 1 fg/ μ L concentration and 4-nonylphenol and 4-nonylphenol monoethoxylate were detected
- Diethyl terephthalate, di-isobutyl phthalate, di-butyl phthalate were all detected in the real-world plastic samples while nonylphenols were only detected in the bag and wrap.
- One of the main difficulties with this analysis is minimizing background from plastic during the sample prep and sample introduction. Dimethyl phthalate was still observed in the blank even with rigorous cleaning.

Reference

1. Votavová, L. *et al.* Migration of Nonylphenols from Polymer Packaging Materials into Food Simulants. *Czech Journal of Food Sciences* **2009**, 27, 293–299. 10.17221/152/2008-CJFS.

Analysis of PAHs Using Hydrogen Carrier Gas and the Hydrogen-Optimized Source with GC/MS and GC/MS/MS in Challenging Soil Matrix

Authors: Samuel Haddad, Bruce Quimby, Anastasia Andrianova, Erinn Oneill, and Eric Fausett
Agilent Technologies, Little Falls Site, Wilmington, Delaware

Introduction

Polycyclic aromatic hydrocarbons (PAHs) are a group of chemical compounds that are composed of two or more fused conjugated benzene rings with a pair of carbon atoms shared between rings in their molecules. Further, PAHs originate from multiple sources and are widely distributed as contaminants throughout the world. The most common way to detect PAHs is with GC/MS on the single or triple quadrupole instrument. Helium is the preferred carrier gas for GC/MS analysis; however, its reoccurring shortages and mounting costs have increased demand for applications using hydrogen as the carrier gas. This application focuses on the analysis of 27 PAHs on a triple quadrupole GC/MS in multiple reaction monitoring (MRM) mode using hydrogen carrier gas, the HydroInert source, and mid-column backflush to address heavy matrix. A liquid-extracted soil sample was used as a worst-case scenario to test the Ultra Inert mid-frit inlet liner and the method for PAH analysis. Liner, column, and system robustness were demonstrated by 500 repeat injections of extracted soil sample.

Experimental

Chemicals and reagents

PAH calibration standards (part number G3440-85009) were diluted using isooctane. Twelve calibration levels were prepared: 0.1, 0.25, 0.5, 1, 2, 10, 20, 100, 200, 400, 750, and 1,000 ng/mL. Each level also contained 500 ng/mL of the ISTDs.

Matrix sample preparation

Commercial topsoil (Weaver Mulch, Coatesville, PA, U.S.) was dried at 120 °C overnight. A 5 g sample of the dried soil was extracted with 30 mL dichloromethane/acetone (1:1 v/v) with agitation overnight. The extract was filtered, and the filtrate was reduced 7.5 fold in volume by evaporation. The resulting extract was spiked with 100 ppb of the 27 PAH analytes and 500 ppb of the five ISTD compounds.

Robustness testing

Calculated concentration stability was tested over 500 replicate injections using spiked soil extract. After every 100 injections, the liner and septa were replaced. After every 300 injections, the split/splitless inlet gold seal was replaced.

Instrumentation

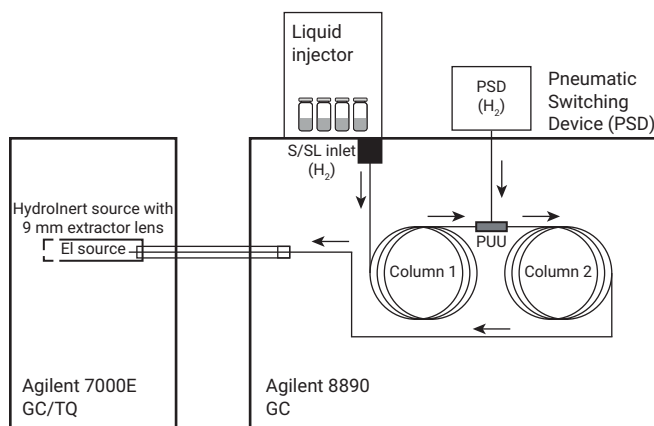


Figure 1. GC/MS/MS configuration.

Table 1. Experimental parameters.

Agilent 8890 GC with Fast Oven, Auto Injector, and Tray	
Injection Volume	1.0 µL
Inlet	EPC split/splitless
Mode	Pulsed splitless
Injection Pulse Pressure	40 psi until 0.7 min
Purge Flow to Split Vent	50 mL/min at 0.75 min
Septum Purge Flow Mode	Standard, 3 mL/min
Inlet Temperature	320 °C
Oven	Initial: 60 °C (1 min hold) Ramp 1: 25 °C/min to 200 °C Ramp 2: 10 °C/min to 335 (4.4 min hold)
Column 1	Agilent J&W DB-EUPAH, 20 m × 0.18 mm, 0.14 µm
Control Mode	Constant flow, 0.9 mL/min
Inlet Connection	Split/Splitless Inlet
Outlet Connection	Purged Ultimate Union (PUU)
Post-run Flow (Backflushing)	– 5.274 mL/min
Column 2	Agilent J&W DB-EUPAH, 20 m × 0.18 mm, 0.14 µm
Control Mode	Constant flow, 1.1 mL/min
PSD Purge Flow	3 mL/min
Inlet Connection	Purged Ultimate Union (PUU)
Outlet Connection	Agilent 7000E GC/TQ
Post-run Flow (Backflushing)	5.443 mL/min
Agilent 8890 GC Backflush Parameters	
Inlet Pressure (Backflushing)	2 psi
Backflush Pressure	80 psi
Void Volumes	7.2
Backflush Time	1.5 min
Agilent 7000E GC/TQ	
Source	Agilent HydroInert source
Drawout Lens	9 mm
Transferline Temperature	320 °C
Source Temperature	325 °C
Quadrupole Temperature	150 °C
Mode	Dynamic MRM
EM Voltage Gain	10
Solvent Delay	5.5 min
Collision Gas	Nitrogen (only), 1.5 mL/min
Automatically Subtract Baseline	Yes
Advanced SIM/MRM Thresholding	Yes
Tune File	atunes.eiex.jtune.xml

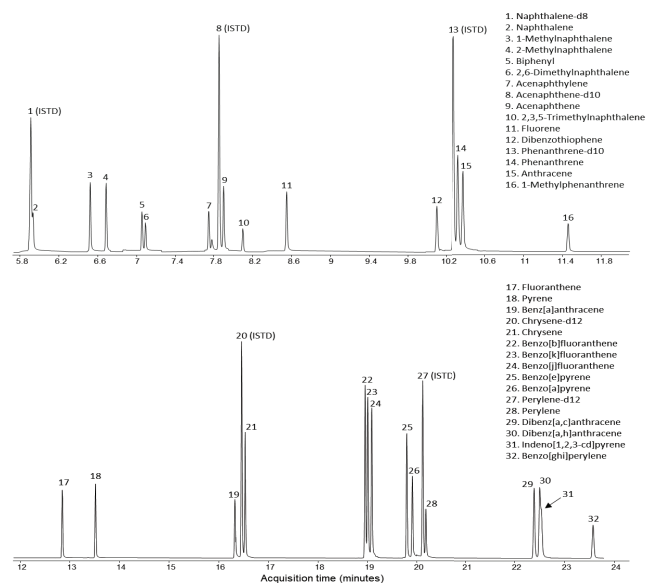


Figure 2. MRM TIC of 27 PAHs at 100 pg/µL and 5 ISTDs at 500 pg/µL.

Table 2. 12-level MRM ISTD calibration curve with a range of 0.1 to 1,000 pg. MDLs were defined as $MDL = t(n - 1, 0.99) \times SD$, where $t(n - 1, 0.99)$ is the one-sided Student's t-statistic at the 99% confidence limit for $n - 1$ degrees of freedom, (2.998 for $n = 8$), and SD is the standard deviation of replicate solvent samples spiked at 0.25 pg. (Continued on next page)

Analyte	Linear Range (pg)	Correlation Coefficient (R ²)	MDL (pg)
Naphthalene	0.1 to 1,000	0.9999	0.07
1-Methylnaphthalene	0.1 to 1,000	0.9995	0.09
2-Methylnaphthalene	0.1 to 1,000	0.9995	0.06
Biphenyl	0.1 to 1,000	0.9994	0.16
2,6-Dimethylnaphthalene	0.1 to 1,000	0.9994	0.10
Acenaphthylene	0.25 to 1,000	0.9996	0.15
Acenaphthene	0.1 to 1,000	0.9996	0.13
2,3,5-Trimethylnaphthalene	0.1 to 1,000	0.9994	0.10
Fluorene	0.1 to 1,000	0.9996	0.05
Dibenzothiophene	0.1 to 1,000	0.9995	0.10
Phenanthrene	0.1 to 1,000	0.9997	0.09
Anthracene	0.1 to 1,000	0.9996	0.15
1-Methylphenanthrene	0.1 to 1,000	0.9996	0.08
Fluoranthene	0.1 to 1,000	0.9995	0.03
Pyrene	0.1 to 1,000	0.9998	0.08
Benz[a]anthracene	0.1 to 1,000	0.9995	0.13
Chrysene	0.1 to 1,000	0.9996	0.11
Benzo[b]fluoranthene	0.1 to 1,000	0.9995	0.06
Benzo[k]fluoranthene	0.1 to 1,000	0.9999	0.09
Benzo[j]fluoranthene	0.1 to 1,000	0.9999	0.12
Benzo[e]pyrene	0.1 to 1,000	0.9997	0.07
Benzo[a]pyrene	0.1 to 1,000	0.9998	0.11
Perylene	0.1 to 1,000	0.9996	0.11

Table 2. 12-level MRM ISTD calibration curve with a range of 0.1 to 1,000 pg. MDLs were defined as $MDL = t(n - 1, 0.99) \times SD$, where $t(n - 1, 0.99)$ is the one-sided Student's t-statistic at the 99% confidence limit for $n - 1$ degrees of freedom, (2.998 for $n = 8$), and SD is the standard deviation of replicate solvent samples spiked at 0.25 pg. (Continued from previous page).

Analyte	Linear Range (pg)	Correlation Coefficient (R^2)	MDL(pg)
Dibenz[a,c]anthracene	0.1 to 1,000	0.9997	0.05
Dibenz[a,h]anthracene	0.1 to 1,000	0.9994	0.09
Indeno[1,2,3-cd]pyrene	0.1 to 1,000	0.9996	0.08
Benzo[ghi]perylene	0.1 to 1,000	0.9997	0.06

Results and discussion

GC/MS methodology

Figure 2 shows the MRM total ion chromatogram (TIC) of the 100 pg/ μ L calibration standard with 500 pg/ μ L ISTDs. Using these parameters, the peak shapes for PAHs—especially the latest ones—are excellent. In general, the HydroInert source provided the best peak shapes for PAHs when using hydrogen carrier gas.

Table 2 shows the calibration results of the system with 12 calibration levels from 0.1 to 1,000 pg. All analytes show excellent linearity across the entire range. Using the HydroInert source also resulted in excellent signal-to-noise ratios, allowing the calibration range to be extended to subpicogram levels. Of the 27 analytes, 26 had sufficient signal for calibration from 0.1 to 1,000 pg. One was calibrated from 0.25 to 1,000 pg.

One of the problems encountered when using helium carrier gas and the standard 3 mm EI source extractor lens for the analysis of PAHs is that the response of ISTDs climbed with increasing concentration of the analytes. This effect can cause the response of perylene-d12 to increase by as much as 60% over the calibration range and cause significant errors in quantitation. Figure 3 shows the ISTD response stability over the calibration range with the current method. As demonstrated in Figure 3, the use of hydrogen carrier gas with the HydroInert source and a 9 mm extractor lens also eliminates the creeping ISTD response problem. The %RSD for the raw area responses across the calibration range are all 6.4% or less. This is important for achieving the excellent calibration linearity shown in Table 2.

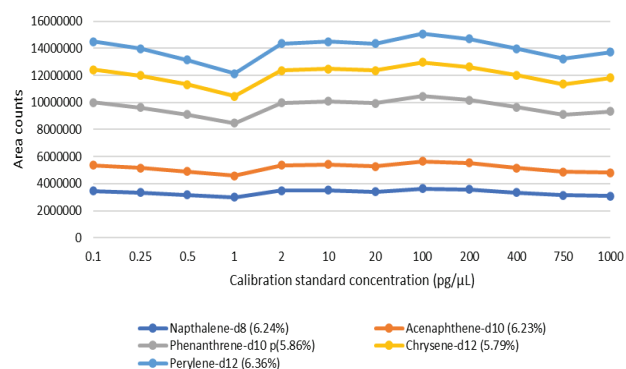


Figure 3. ISTD response over calibration range.

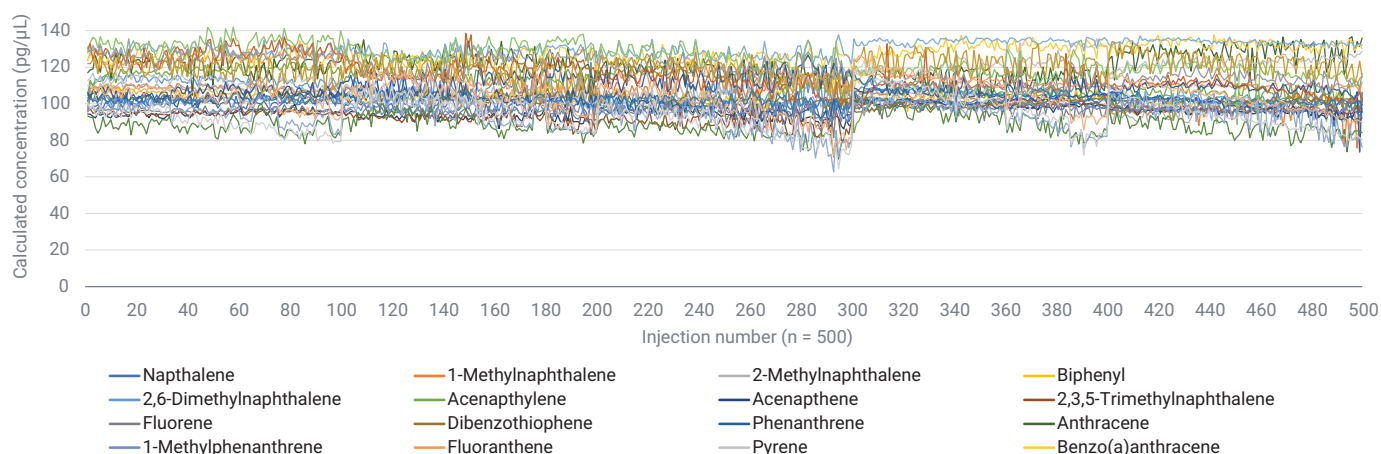


Figure 4. Stability of calculated concentrations over 500 injections of soil matrix spiked with 100 pg PAH standard and 500 pg of ISTD.

Method robustness in complex matrix

The stability of calculated concentration over 500 injections is presented in Figure 4. For 23 of 27 analytes, the response is stable, where the RSDs for each set of 100 injections are under 5%. However, the calculated concentrations start to decline for dibenz[a,c]anthracene, dibenz[a,h]anthracene, indeno[1,2,3-cd]pyrene, and benzo[ghi]perylene around injection 70 (in a sequence of 100) and RSDs are slightly higher than 5% for each set of 100 injections. Over all 500 injections, with routine maintenance and backflush, injection RSDs were <12% for all analytes. This demonstrates excellent quantitation stability while continuously challenging the system with a complex soil extract. After each set of 100 injections, the liner and septa were replaced, which resulted in the concentration for dibenz[a,c]anthracene, dibenz[a,h]anthracene, indeno[1,2,3-cd]pyrene, and benzo[ghi]perylene to recover back to starting concentrations. The UI mid-frit liner performed well at trapping complex matrix. The observation of a decline in concentration at approximately injection 70 for the four late-eluting compounds demonstrates that the liner was becoming saturated with matrix. As the liner saturates, the transfer of late-eluting compounds becomes inhibited.

Conclusion

The triple quadrupole GC/MS method for analyzing PAHs using hydrogen carrier gas, the Agilent HydroInert source, and backflush described here demonstrated several improvements over previous hydrogen and helium methods:

- Excellent chromatographic peak shape with little or no tailing
- MDL and linearity comparable to or better than obtained with helium
- Better chromatographic resolution with a shorter run time
- ISTD response stability across four orders of calibration
- Excellent linearity over 0.1 to 1,000 pg for 26 out of 27 analytes
- Average MDL of 0.09 pg for 27 analytes
- Reliable and accurate quantitation over 500 injections of a challenging soil extract with routine maintenance
- Excellent performance of the Agilent universal Ultra Inert mid-frit inlet liner when analyzing challenging soil matrix

For those laboratories looking to change their PAH analysis to the more sustainable hydrogen carrier gas, the HydroInert source with the 9 mm extractor lens enables the transition with equivalent or better performance.

Reference

1. Haddad, S. P.; Quimby, B. D.; Andrianova, A. A. GC/MS/MS Analysis of PAHs with Hydrogen Carrier Gas Using the Novel Agilent HydroInert Source in a Challenging Soil Matrix, *Agilent Technologies application note*, publication number 5994-5776EN, **2023**.

Automated Sample Preparation Using CTC PAL3 to Analyze >570 Pesticides in an Orange by the Combination of GC/MS/MS and LC/MS/MS Techniques

Authors: Zhiming, Zhang; Ge, Meng; Zhicong, Wang; Jianguo, Ji;
Chunxiao, Wang, Lorna De-Leoz
Agilent Technologies, Inc., Shanghai, P.R. China

Introduction

Automated sample preparation can not only increase testing efficiency, but also reduces dependency on in-person activity. For example many lab chemists had to stay at home due to COVID-19 pandemic, resulting in a lot of sample testing been delayed due to the shortage of chemist availability. Compared with manual work, an automated workflow, especially coupled online to mass spectrometry, is less worker-reliant and a best choice to tackle this kind of situation.

The manual sample preparation process for QuEChERS includes solvent extraction, salting and cleaning, with multi-time of shaking/vortex and centrifugation. This process avoids dependency on chemist time and increases the precision of the results due to reducing human error.

An automated workflow was developed to analyze multiclass pesticides in oranges with the combination of GC/MS/MS and LC/MS/MS techniques. Sample preparation was automatically done with CTC PAL3 on the basis of QuEChERS, which ensured consistent and high quality results. Using scripts, the sample preparation was done in overlapped mode, avoiding additional sample prep overhead time.

Validations were done at three different spiking levels (10, 20, and 50 µg/kg) with 5 replicates for each level. The validation results for automatic sample preparation and manual sample preparation were summarized and compared.

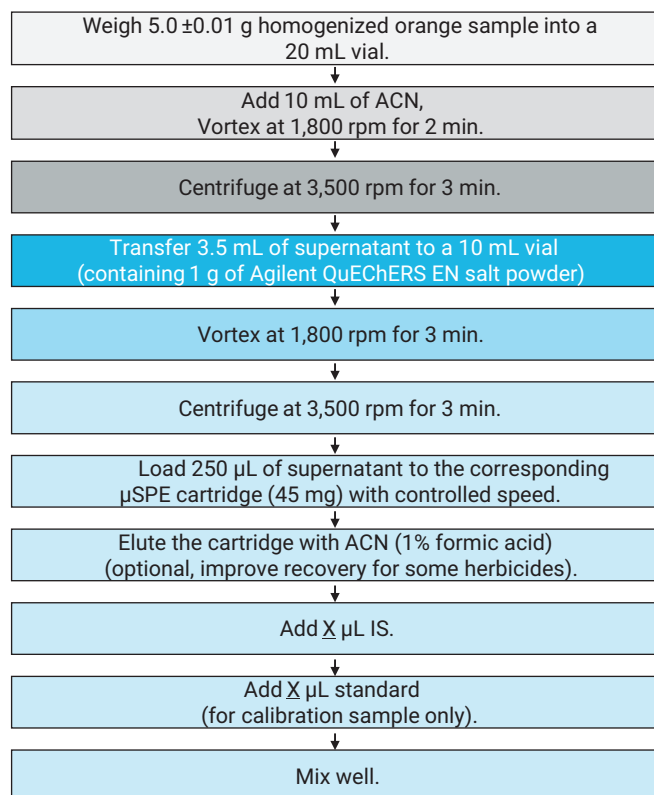


Agilent 1290 Infinity II LC + 6470

Figure 1. Instruments used in the experiment.

Experimental

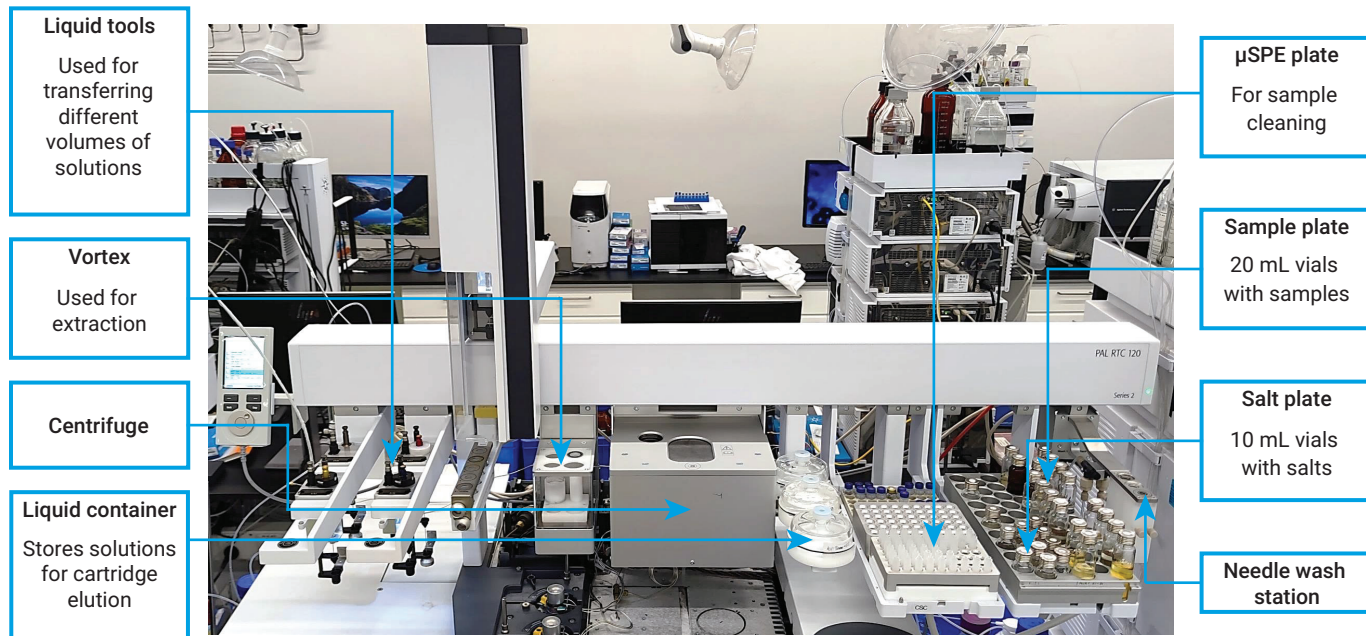
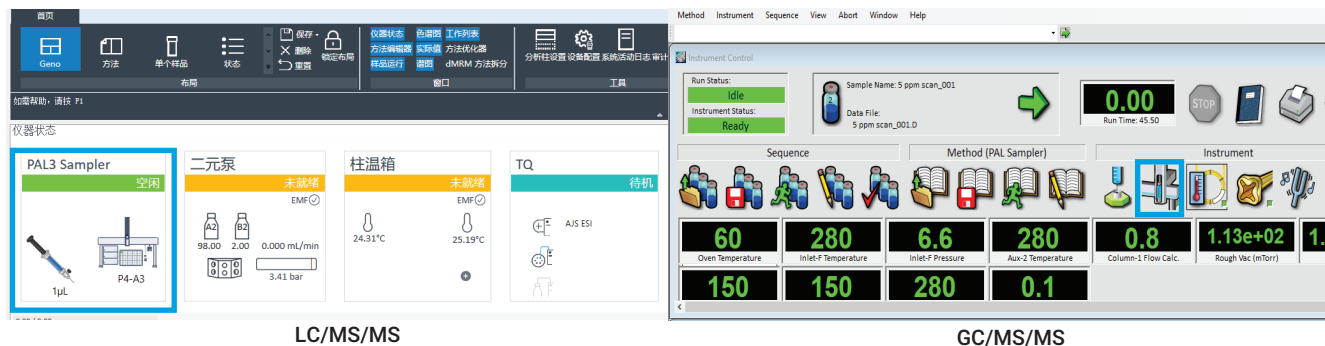
Automatic sample preparation



Partial parameters of PAL3 auto sample preparation

Conditioning		Internal Standard	
Conditioning Solvent Source	none	Internal Standard Source	none
Conditioning Solvent Index	2	Internal Standard Index	54
Conditioning Solvent Volume	100 μ L	Internal Standard Volume	7.7 μ L
Conditioning Solvent Fill Speed	10 μ L/s	Internal Standard Fill Speed	1 μ L/s
Sample μSPE		Solvent Addition	
μ SPE Sample Load Volume	257 μ L	Solvent Source	none
μ SPE Sample Fill Speed	5 μ L/s	Solvent Index	1
Elution		Solvent Volume	16.45 μ L
Elution Solvent Source	none	Solvent Fill Speed	5 μ L/s
Elution Solvent Index	2	Target Standard	
Elution Volume	100 μ L	Target Standard Source	none
Elution Solvent Fill Speed	5 μ L/s	Target Standard Index	52
Protectants		Target Standard Volume	3.85 μ L
Protectant Source	none	Target Standard Fill Speed	1 μ L/s
Protectant Index	3	Mixing	
Protectant Volume	0 μ L	Mix Cycles	5
Protectant Fill Speed	5 μ L/s	Mix Volume	500 μ L
		Injection	

Instrument control panel



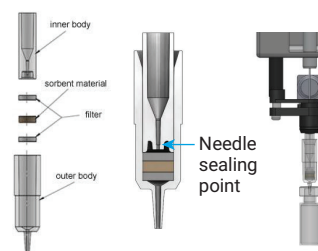
Liquid tools



Centrifuge



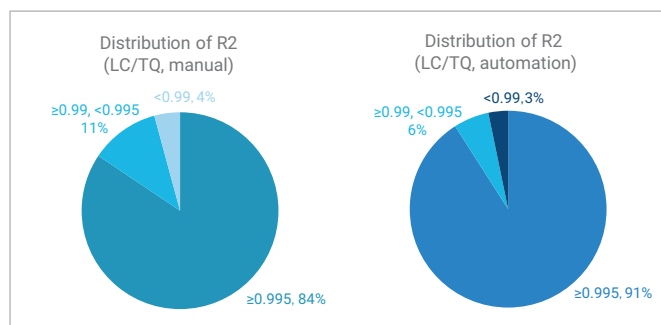
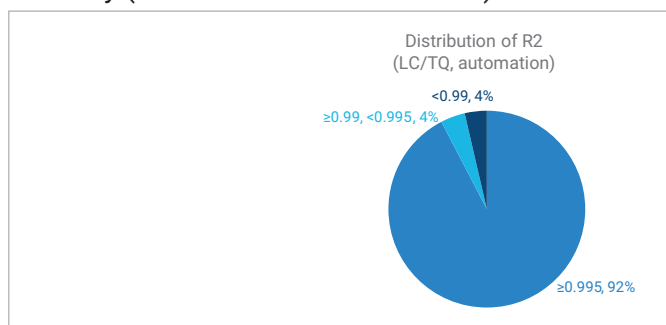
Vortex



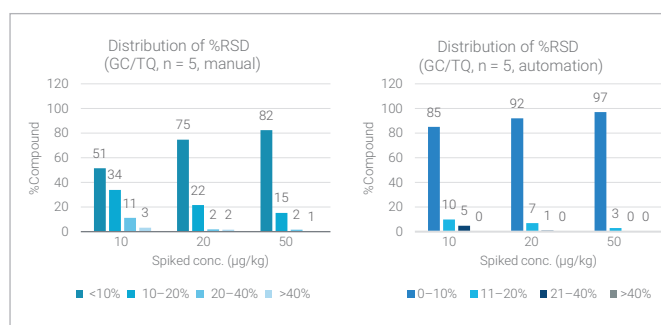
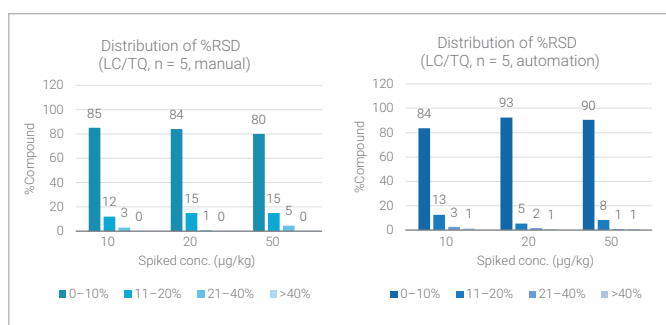
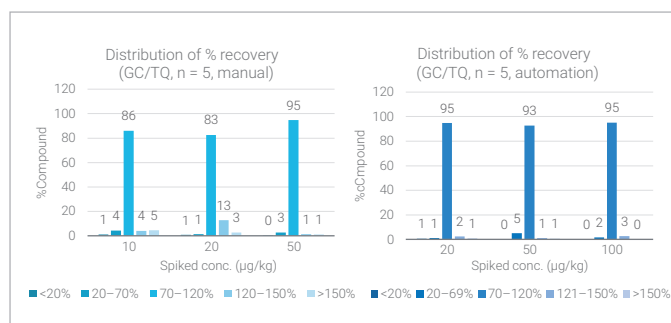
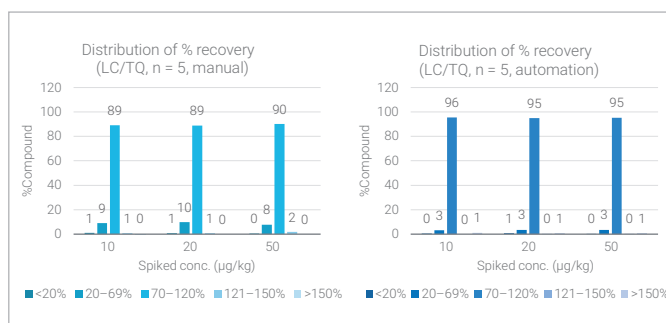
Design of μ SPE

Results and discussion

Linearity (manual versus automation)



Accuracy (manual versus automation)



Conclusion

Full automation, high efficiency, low cost

An automatic sample preparation workflow for analyzing >570 pesticides in an orange using the combination of GC/MS/MS and LC/MS/MS techniques was developed for the first time.

In general, automatic workflow has better performance than manual workflow by comparison of linearity, accuracy and repeatability of validation results done by manual and automated sample preparation.

References

1. GB2763-2021: National Food Safety Standard- Maximum Residue Limits for Pesticides in Food.
2. GB23200.121-2021: National Food Safety Standard- Determination of 331 Pesticides and Metabolites Residues in Foods of Plant Origin-LC/MS/MS.
3. GB23200.121-2018: National Food Safety Standard- Determination of 208 Pesticides and Metabolites Residues in Foods of Plant Origin-GC/MS/MS.

Achieving the MRLs with Hydrogen Carrier Gas: GC/MS/MS Analysis of 200 Pesticides in Produce

Authors: Anastasia Andrianova, Eric Fausett, Bruce Quimby, Limian Zhao, Joel Ferrer, and Aaron Boice
Agilent Technologies, Inc.

Introduction

Arising need for analyzing pesticides with hydrogen

Recurring helium shortages and increased prices drive the demand for performing GC/MS analysis with alternative carrier gasses. While helium is the best carrier gas for GC/MS, hydrogen is the second-best alternative. However, unlike helium, hydrogen is not an inert gas. Hence, it could react with target analytes resulting in compound degradation, chromatographic problems such as peak tailing, distorted ion ratios in the mass spectrum, poor library matching, and sensitivity loss.

Pesticides analysis can be challenging even with He carrier gas given the diverse and labile nature of many pesticides and complex matrices, in which they are analyzed. This work discusses the key strategies for analyzing pesticides with H₂ carrier gas while delivering high-quality uncompromised results.

Experimental

Key considerations for successful transitioning GC/MS/MS analysis from helium to hydrogen

It is important to recognize the differences with using hydrogen carrier. The EI GC/MS Instrument Helium to Hydrogen Carrier Gas Conversion Guide¹ provides detailed instructions for method conversion from He to H₂ carrier. The user guide outlines considerations and procedures for H₂ safety necessary to make the transition to H₂ carrier gas successful.

Additional factors complicating pesticide residue analysis include low tolerance limits that require high sensitivity of the analysis, thermal lability, chemical diversity, and interferences arising from complex matrices. This work leveraged the key practices that enhance pesticide residue analysis with GC/MS/MS applicable to both He and H₂ carrier gas outlined elsewhere.² Among those best practices were effective sample extraction and matrix cleanup, midcolumn backflushing, and the use of the temperature-programmed injection in solvent vent mode with a 2 mm dimpled liner (without glass wool).

The instrument conditions are summarized below:

- Solvent vent injection: 2 µL, 2 mm dimpled liner, 60 °C for 0.1 minutes, then to 280 °C at 600 °C/min
- Two Agilent HP-5ms UI 20 m (0.18 mm × 0.18 µm) columns connected with the purged ultimate union (PUU)
- Oven program: 60 °C for 1 minute, then to 170 °C at 40 °C/min, 0 minutes hold, then to 310 °C at 10 °C/min, hold for 2.25 minutes.
- Column flows: 1.1 and 1.3 mL/min; H₂ carrier gas

Results and discussion

Maintaining the retention times and chromatographic resolution with hydrogen carrier gas

The combination of method translation followed by retention time locking allowed for transferring the conventional 20-minute analysis of 203 pesticides with He to H₂ carrier gas, while maintaining the relative elution order and precisely matching the retention times (Figure 1). The same techniques were also used to translate the 20-minute analysis to 10 minutes with hydrogen carrier gas (Figure 1, bottom). Chromatographic resolution achieved with H₂ and the 20-minute analysis surpassed that with He, enabling better separation between the targets and the coeluting interferences from the complex spinach matrix. The resolution with a 10-minute analysis and H₂ was comparable to that with He and 20-minute analysis.

Does spectrum distortion happen with hydrogen? No, if using the hydrogen-optimized EI source hardware

H₂ carrier gas provides advantages for chromatographic separation. However, it could present a challenge for detection with a mass spectrometer. Due to its reactivity, H₂ carrier gas can alter the spectrum for compounds susceptible to reacting with hydrogen. Figure 2A shows the distorted mass spectrum for tecnazene, a fungicide used to control dry rot, acquired with the conventional EI source. Using the hydrogen-optimized HydroInert source and the HES source allows for maintaining the same ion ratios as observed with helium carrier gas (Figures 2B and 2C). Minimizing in-source reactions with H₂, allows for using the existing spectral libraries for identity confirmation and the MRM transitions developed with He for reliable quantitation.

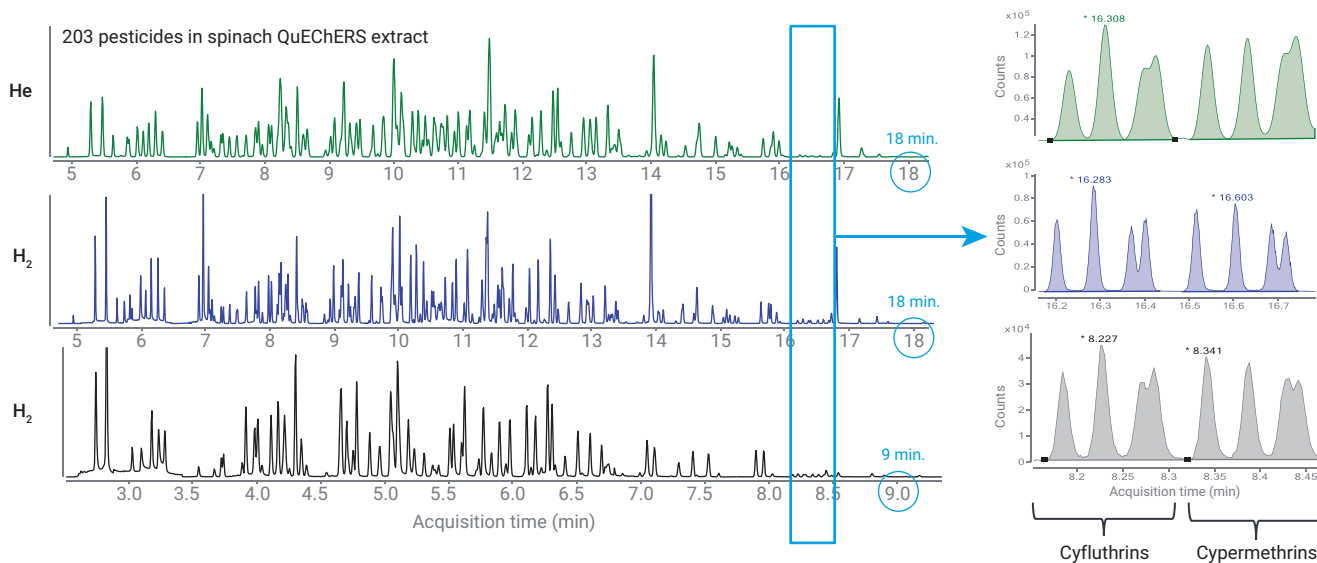


Figure 1. MRM Chromatograms of 203 pesticides in spinach QuEChERS extract analyses with He and H₂ carrier gases.

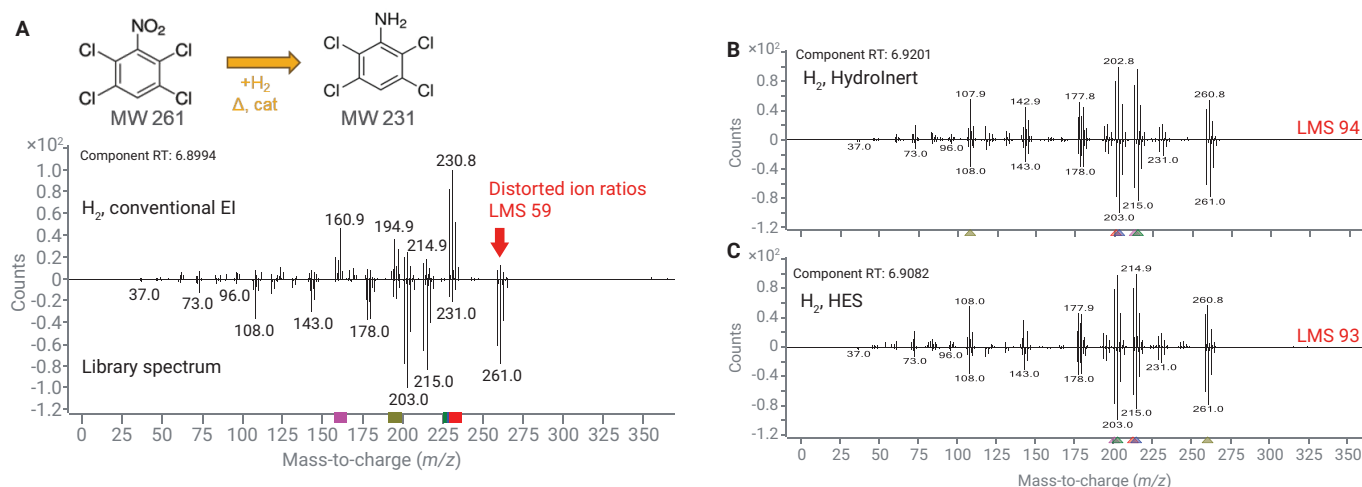


Figure 2. Spectra acquired for tecnazene with H_2 and (A) conventional EI, (B) HydroInert, and (C) HES compared to the NIST library.

Distorted ion ratios lead to decreased sensitivity

The extent of GC/MS/MS sensitivity reduction with H_2 compared to He varies if the target is susceptible to reacting with H_2 . Compounds that do not interact with H_2 show 2 to 5 times higher detection limits with H_2 than with He. For compounds susceptible to reacting with H_2 (as can be confirmed by the distorted spectrum), sensitivity can be reduced over 100 times.

For example, tecnazene, which spectra were shown in Figure 2, demonstrates sensitivity reduction over 100 times when using the conventional EI source with H_2 (Figure 3B versus 3A). This can be attributed to the reduction of the molecular ion and the MRM precursor m/z 261 with the conventional source.

By using the HydroInert or the HES EI sources and minimizing the in-source reactions, the sensitivity of analysis is restored to the levels comparable to those with He. Figures 3C and 3D show that tecnazene can be reliably quantitated below the default MRL of 10 ppb with both the HydroInert and the HES source. Such sensitivity cannot be achieved when using the conventional EI source with H_2 .

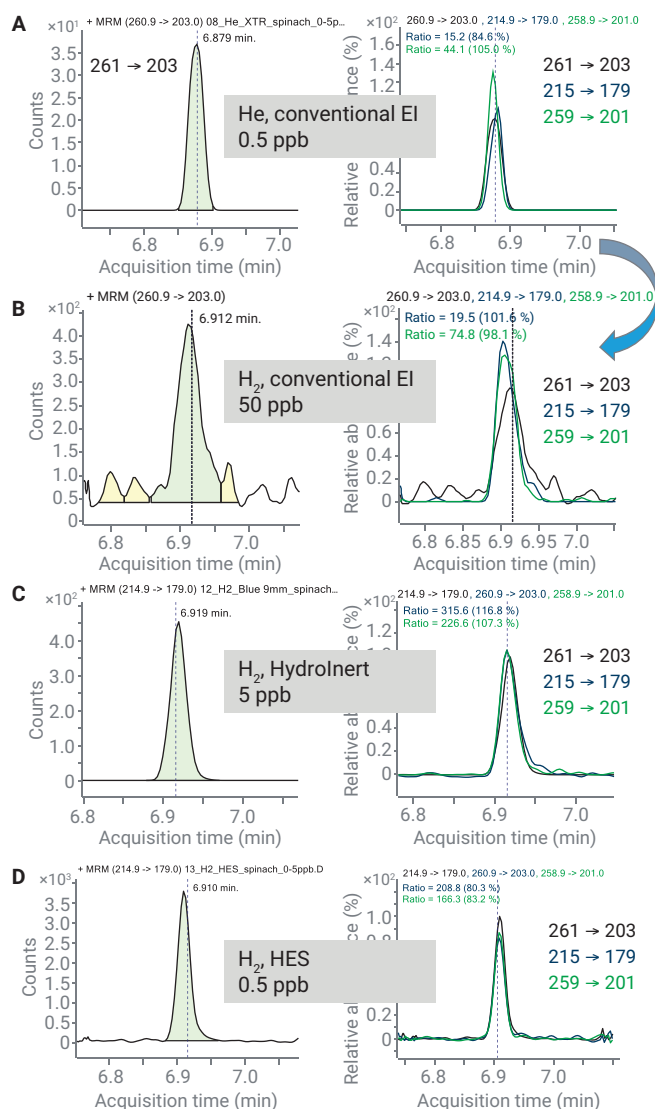


Figure 3. MRM chromatograms for tecnazene acquired with He and H_2 .

Compounds with diverse chemical structures react with H₂ resulting in spectral distortion

Evaluating an analyte's mass spectrum with H₂ is the simplest way to determine if the target undergoes undesirable chemical transformation in the EI source. If the spectrum appears distorted, then difficulties with compound quantitation are expected. In this case, the MRMs would need to be re-optimized, and quantitation accuracy may still suffer due to the uncontrolled and nonreproducible chemical transformations in the source. Table 1 shows library match scores for 15 pesticides that demonstrated in-source reactivity with hydrogen when a conventional EI source was used. The library match scores and ion ratios were restored with the Hydrolnert source and mostly restored with the HES source.

Calibration performance in spinach QuEChERS extract

The developed 20-minute GC/MS/MS analysis method using Hydrolnert and HES sources was applied the analysis of 203 pesticides in spinach QuEChERS extract. The calibration results are summarized in Figure 4. The blue (Hydrolnert) and green (HES) bars correspond to the number of compounds (out of 203) which had a given parameter.

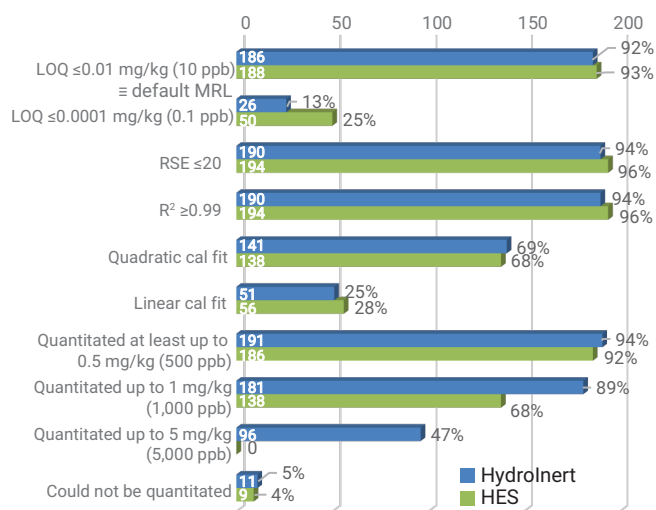


Figure 4. Calibration results.

Table 1. Library match scores for 15 pesticides.

Pesticide/EI Source Type	RT (min)	Helium Carrier Gas		Hydrogen Carrier Gas		
		Conventional EI Source	High Efficiency Source	Conventional EI Source	Hydrolnert EI Source	High Efficiency Source
Tecnazene	6.915	82	84	59	94	93
BHC alpha isomer	7.623	98	98	81	93	96
Dichloran	7.783	89	93	67	90	89
BHC beta isomer	8.019	97	97	77	92	96
Pentachloronitrobenzene	8.212	91	93	67	91	95
BHC delta isomer	8.502	90	94	74	87	94
Heptachlor	9.328	91	88	74	87	93
Malathion	9.742	90	90	56	84	76
Bromophos-ethyl	11.037	93	90	62	87	92
Prothiofos	11.510	95	94	65	92	91
Profenofos	11.561	91	87	66	90	85
Sulprofos	12.666	98	88	61	87	91
Edifenphos	12.953	92	94	59	92	77
Tebuconazole	13.292	93	92	66	89	76
Piperonyl butoxide	13.402	92	94	68	92	79

Conclusion

Pesticides can be analyzed with H₂ at or below MRLs

However, just like with He, some pesticides may be more challenging to analyze at low concentrations.

- Over 90% of targets could be quantitated at or below 10 ppb (mg/kg) in spinach extract, which is the default MRL.
- Using the optimized GC conditions (injection, column set) and suitable MS EI source is essential when using H₂.
- The Hydrolnert source provides improved sensitivity compared to the conventional EI source and best spectral fidelity.
- HES provides best sensitivity and good spectral fidelity.

References

1. Agilent EI GC/MS Instrument Helium to Hydrogen Carrier Gas Conversion. *Agilent Technologies user guide*, publication number 5994-2312EN, **2022**.
2. Five Keys to Unlock Maximum Performance in the Analysis of Over 200 Pesticides in Challenging Food Matrices by GC/MS/MS, *Agilent Technologies application note*, publication number 5994-4965EN, **2022**.

Accurate Mass Library for PFAS Analysis in Environmental Samples Using High-Resolution GC/Q TOF

Authors: Sofia Nieto¹, Matthew Giardina¹, Matthew Curtis¹,
Luann Wong², Gabrielle Black², Thomas Young², Charles Yang¹

¹ Agilent Technologies, Santa Clara, CA

² Department of Civil and Environmental Engineering,
University of California, Davis, CA

Introduction

Per- and polyfluoroalkyl substances (PFAS) are emerging contaminants of increasing concern due to their environmental persistence, toxicity, and capability of bioaccumulation. There are currently thought to be over 6,000 PFAS that have been commercially produced and recent studies have shown that many emerging PFAS that have been detected in the environment can be volatile or semi-volatile in nature. Therefore, a variety of analytical techniques are necessary for their detection. GC/MS is typically used for detecting volatile and nonpolar PFAS compounds. In this study, a GC/Q-TOF system was used to take advantage of high resolution for detecting compounds with mass defect that is different from that of complex environmental matrices. For specific and sensitive PFAS detection in soil and drinking water, an accurate mass GC/MS library has been created. Other contaminants in drinking water such as disinfection byproducts, industrial chemicals originated from personal care products, drugs, and pesticide residues were also identified.

Experimental

GC-amenable PFAS standards have been used to obtain accurate mass spectra. Soil was sampled from two fields in California that have historically received biosolids and extracted with methylene chloride. The drinking water samples were collected at two different locations in California and represented two different water source categories: a small surface water (Weaverville) and a mixed surface and ground water (Irvine). Water samples (2.4 L) were extracted on a multimode SPE (HLB, WAX,

WCS, Isoelut ENV) and eluted with 5% MTBE in MeOH, DCM, 0.5% NH₄OH in 1:1 EtAC:MeOH, and 1.7% formic acid in 1:1 EtAC:MeOH. The combined extracts were concentrated, solvent exchanged to EtAC and diluted 10x. GC/MS analysis was performed using an Agilent 8890 GC coupled to an Agilent 7250 high resolution Q-TOF (Figure 1) using the following the data acquisition parameters (Table 1).



Figure 1. Agilent 7250 GC/Q-TOF

Table 1. GC/Q-TOF Acquisition Parameters

GC and MS Conditions	Agilent DB-5ms	Agilent DB-624
MS	Agilent 7250 Q-TOF	
GC	Agilent 7890	
Inlet	MMI, 4 mm UI liner single taper with wool	
Inlet Temperature	70 °C for 0.01 min; 300 C/min to 250 °C	
Injection Volume	1 µL	
Columns	Agilent DB-5ms UI, 30 m × 0.25 mm, 0.25 µm	Agilent DB-624 UI, 30 m × 0.25 mm, 1.4 µm
Oven Temperature Program	35 °C for 2 min, 7 °C/min to 210 °C, 20 °C/min to 300 °C, 4 min hold	30 °C for 2 min, 3 °C/min to 75 °C, 2 °C/min to 110 °C, 10 °C/min to 210 °C, 20 °C/min to 240 °C, 2 min hold
Column Flow	1.2 mL/min constant flow	1 mL/min constant flow
Carrier Gas	Helium	
Transfer Line Temperature	250 °C	
Quadrupole Temperature	150 °C	
Source Temperature	200 °C	
Electron Energy	70 eV	
Emission Current	Variable by time segment, 0.01 to 5 µA	
Spectral Acquisition Rate	5 Hz	
Mass Range (Tune)	50 to 1,200 <i>m/z</i>	

The chromatographic deconvolution and library search were performed in the MassHunter Unknowns Analysis 11.1. Accurate mass EI fragments were converted to the theoretical *m/z* using MassHunter Qualitative Analysis software version 10.0, and the spectra were exported into the accurate mass Personal Compound Database and Library (PCDL) Manager version 8.0. The PCDL for PFAS, PCDL for Pesticides and Environmental contaminants, as well as NIST 20 were used to perform initial compound identification. Retention indices and accurate mass information were used to confirm the compound ID. Statistical analysis was performed in Mass Profiler Professional (MPP) 15.1.

Results and discussion

Accurate Mass Library for PFAS

In order to create an accurate mass GC/MS PCDL, the spectra have been collected for over a hundred PFAS compounds. Accurate mass fragment ions have been automatically annotated with formulas based on accurate mass information and isotope ratios using MassHunter Qualitative Analysis software (Figure 2). The fragment formula annotations were manually verified, corrected when necessary, and automatically converted to the theoretical *m/z*.

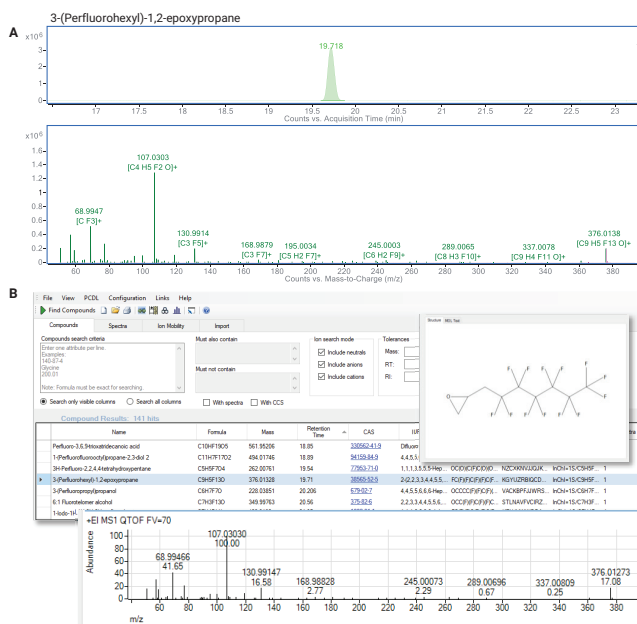
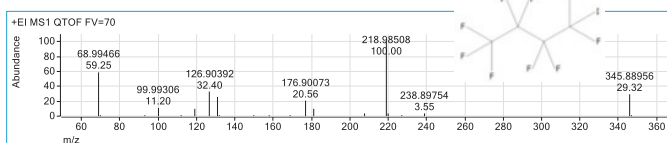


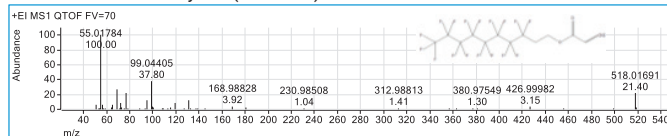
Figure 2. (A) EIC of the molecular ion and fragment formula annotation of spectrum for one of the PFAS compounds in MassHunter Qualitative Analysis software. (B) The PFAS PCDL contains EI spectra as well as the metadata including molecular structure and database identifiers.

The PFAS compound classes include perfluoroalkyl iodides (PFAls), fluorotelomer iodides (FTIs), fluorotelomer alcohols (FTOHs), fluorotelomer olefins (FTOs), fluorotelomer acrylates (FTACs), fluorotelomer methacrylates (FTMACs) and perfluoroalkyl carboxylic acids (PFCAs) among others (Figure 3).

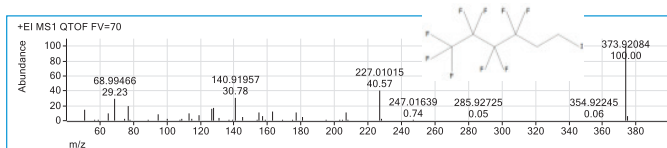
Nonafluoro-1-iodobutane (PFBI)



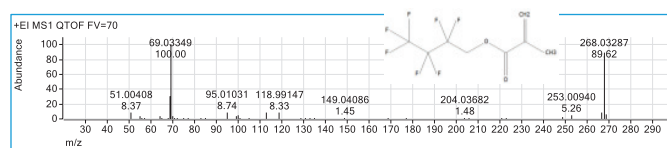
8:2 Fluorotelomer acrylate (8:2 FTAC)



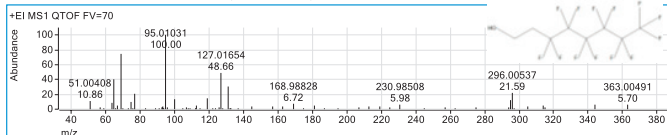
1,1,1,2,2,3,3,4,4-Nonafluoro-6-iodohexane (6:2 FTI)



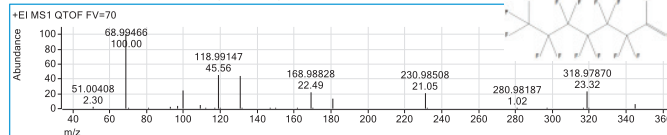
2,2,3,3,4,4,4-Heptafluorobutyl methacrylate (3:1 FTMAC)



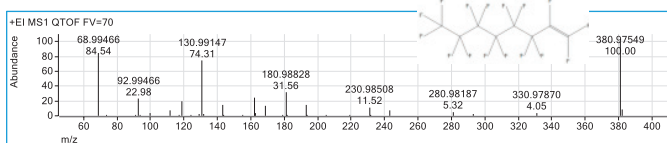
6:2 Fluorotelomer alcohol (6:2 FTOH)



Perfluoroheptanoic acid (PFHpA)



Perfluorooct-1-ene



Methyl perfluorohexanoate

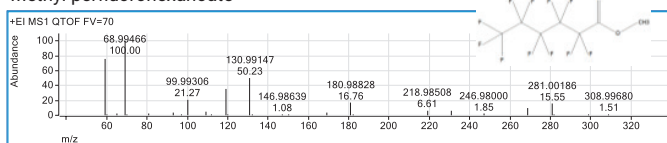


Figure 3. Examples of spectra in PFAS PCDL from different PFAS compound classes.

PFAS in environmental samples

For PFAS detection, the extracts of drinking water and soil were separated on DB-624 column analyzed by the GC/Q-TOF MS. The chromatographic deconvolution was performed in the Unknowns Analysis software using a SureMass algorithm that is optimized for complex high resolution EI data. The PFAS PCDL was used to search the deconvoluted spectra with RT matching. Figure 4 shows PFAS compounds identified in soil and drinking water (one in each matrix). PFAS (a derivative of PFCAs) were detected in most drinking water samples and the soil extract from Field 1.

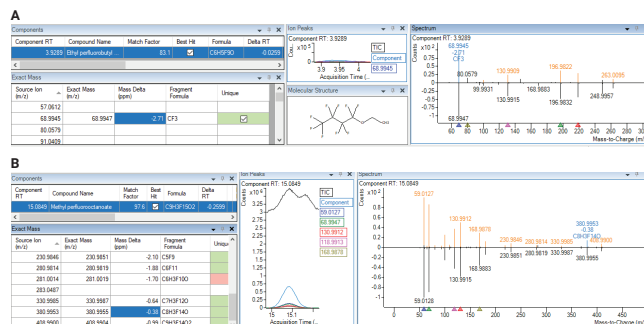


Figure 4. PFAS identified in soil Field 1 (A, ethyl perfluorobutyl ether) and drinking water Irvine (B, Methyl perfluorooctanoate) samples.

Identification of the additional contaminants in drinking water samples

To identify other contaminants in drinking water samples the GC/Q-TOF Pesticide PCDL as well as NIST 20 library were used. Over hundred contaminants have been identified and confirmed using accurate mass information (Figure 5 and Tables 2 and 3) from the sample without reinjection.

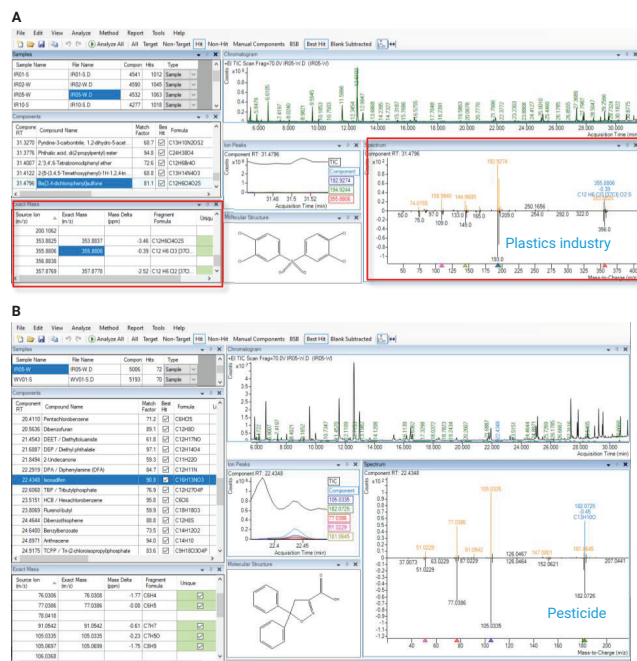


Figure 5. Examples of the contaminants identified in drinking water extracts using NIST 20 (A) and Pesticide PCDL (B). ExactMass tool (highlighted in red) helps to provide additional confirmation of unit mass library hits based on accurate mass. Compound ions are highlighted in the mirror plot when m/z corresponds to the library hit formula.

Table 2. Contaminants identified in drinking water using NIST 20 library with the library match score >75.

*Denotes the cases where delta RI was calculated considering NIST estimated RIs rather than experimental (experimental not available).

RT	Compound Name	Match Score	Formula	RI delta	RT	Compound Name	Match Score	Formula	RI delta	RT	Compound Name	Match Score	Formula	RI delta
4.79	Bromodichloromethane	95.4	CHBrCl ₂	-56	19.96	Acenaphthene	91.2	C ₁₂ H ₁₀	-4	27.31	Diethyl phthalate	92.4	C ₁₆ H ₁₄ O ₄	9
4.81	Chloral	78.8	C ₂ HCl ₃	32	20.18	4-Methylbiphenyl	79.4	C ₁₃ H ₁₂	-4	27.59	10-Anthracenedione	93.2	C ₁₄ H ₈ O ₂	-27
4.91	Dichloroacetanilide	86.4	C ₈ H ₇ Cl ₂ N	-76	20.28	4,4'-Di-tert-butylphenol	90.2	C ₁₄ H ₂₂ O	10	28.21	Octachlorostyrene	88.6	C ₈ Cl ₈	-7
4.95	Chloromethylmethyl sulfide	94	C ₂ H ₅ SCl	-59*	20.56	Diethylbenzofuran	92.4	C ₁₂ H ₁₀	-5	28.36	Cyclopenta[def]phenanthrene	97.2	C ₁₅ H ₁₀	-74*
5.11	Dimethyl disulfide	98.4	C ₂ H ₆ S ₂	-35	21.23	1-Bromodecane	75.7	C ₁₀ H ₂₁ Br	-10	28.51	Cyclic octaatomic sulfur	93.1	S ₈	-18
5.35	Methylidylamine	85.7	C ₂ H ₇ N	-50*	21.45	Diethyltoluamide (DEET)	78.1	C ₁₂ H ₁₇ NO	10	28.53	Drometrizole	82.3	C ₁₃ H ₁₁ N ₃ O	-5
5.47	Bromochloromethane	82.8	CHBrCl	-1	21.69	Methylphthalate	96	C ₈ H ₇ BrO ₄	8	28.54	Fluoranthene	97.8	C ₁₆ H ₁₀	-12
5.95	Dibromodichloromethane	95.5	CH ₂ Br ₂ Cl ₂	-25	21.71	Fluorene	75.3	C ₁₃ H ₁₀	-4	28.57	Phenindione	79	C ₁₆ H ₁₀	-50*
6.01	Tetrachloroethylene	96.5	C ₂ Cl ₄	-12	22.01	2-Methylmercaptobenzothiazole	77.8	C ₈ H ₇ NS ₂	2	28.71	8-Carboxynaphthalene-1-carboxamide	85.5	C ₁₂ H ₉ N ₃ O ₃	135*
6.04	1,1-Dimethyl-3-chloropropanol	88.4	C ₅ H ₁₁ ClO	7	22.43	Benzophenone	94.8	C ₁₃ H ₁₀ O	4	28.91	β-Methylanthraquinone	75.5	C ₁₅ H ₁₀ O ₂	33
6.34	Bromochloroacetanilide	86.2	C ₈ H ₇ BrClN	60*	22.60	Tributyl phosphate	93	C ₁₂ H ₂₇ O ₄ P	7	28.94	Dibenzothiophene sulfoxide	87.2	C ₁₂ H ₈ O ₂ S	N/A
6.59	Dichloroacetic acid methyl ester	89.2	C ₃ H ₄ Cl ₂ O ₂	-7*	23.51	Hexachlorobenzene	97.2	C ₆ Cl ₆	9	29.02	Pyrene	89.3	C ₁₆ H ₁₀	-25
6.84	Dimethyl sulfoxide	93.4	C ₂ H ₆ OS	-42	24.19	9-Fluorenone	97.1	C ₁₃ H ₁₀ O	8	29.34	Azapyrene	78.4	C ₁₅ H ₁₀ N	2
7.67	Trichloromethane	98.2	CHCl ₃	-10	24.26	9-Fluorenyl	93.1	C ₁₃ H ₁₀	-53*	31.04	Benzo[b]naphtho[2,1-d]thiophene	81.3	C ₁₅ H ₁₀ S	34*
8.24	Methyl bromodichloroacetate	77.4	C ₃ H ₄ BrCl ₂ O ₂	-3	24.50	Anthracene	94.4	C ₁₄ H ₁₀	0	29.69	2-Amino-9-fluorenone	83.9	C ₁₃ H ₉ N ₂ O	2*
8.31	Dibromochloromethane	86.6	C ₂ HBr ₂ Cl	64*	24.51	9-Fluorenyl	81.9	C ₁₄ H ₁₀	-75	29.87	Bis(4-chlorophenyl) sulfone	77	C ₁₂ H ₈ Cl ₂ O ₂ S	-1
8.56	1-Bromo-2,2-dimethoxypropane	79.2	C ₅ H ₁₁ BrO ₂	-58	24.91	Tris(2-chloroisopropyl)phosphate	82.2	C ₉ H ₁₈ Cl ₃ O ₄ P	27	30.76	2,2'-Methylene-bis(4-methyl-6-tert-butylphenol)	87.5	C ₂₃ H ₃₂ O ₂	2
10.63	2,2-Dichloroacetamide	83.5	C ₂ H ₃ Cl ₂ NO	-4*	25.02	Benzo[h]quinoline	88.2	C ₁₃ H ₉ N	-2	30.90	Benzo[b]naphtho[1,2-d]thiophene	77.2	C ₁₆ H ₁₀ S	13
10.73	1,2-Dichlorobenzene	98.5	C ₆ H ₄ Cl ₂	9	25.53	4-Diphenyl-4-methyl-2E)-pentene	76.5	C ₁₈ H ₂₀	8	30.94	7-Fluorenyl	89.2	C ₁₇ H ₁₀ O	85
14.12	Naphthalene	81.9	C ₁₀ H ₈	-4	25.55	Benzo[h]quinoline	93.1	C ₁₃ H ₉ N	-53*	31.04	Benzo[b]naphtho[2,1-d]thiophene	81.3	C ₁₅ H ₁₀ S	-16
15.45	Caprolactam	89.6	C ₆ H ₁₁ NO	-3	25.73	Carbazole	76.8	C ₁₂ H ₉ N	-4	31.38	Phthalic acid, di(2-propylpentyl) ester	94.8	C ₂₄ H ₃₈ O ₄	5
16.43	2-Methylphthalene	89.3	C ₁₁ H ₁₀	-1	25.60	Di-sec-butyl phthalate	90.8	C ₁₆ H ₂₂ O ₄	-2	31.48	Bis(4-chlorophenyl) sulfone	82.3	C ₁₂ H ₈ Cl ₂ O ₂ S	3*
16.64	Phthalic anhydride	92.5	C ₈ H ₄ O ₃	5	26.09	2,3-Diphenyl-2-propenenitrile	77	C ₁₅ H ₁₁ N	30*	31.51	Bumetizole	78.6	C ₁₇ H ₁₈ Cl ₃ N ₃ O	57
16.98	Benzamide	82.8	C ₇ H ₇ NO	18	26.27	3-Methylbenzothiothiophene	80.8	C ₁₃ H ₁₀ S	-5	31.82	Benzo[a]anthracene-7,12-dione	76.1	C ₁₈ H ₁₀ O ₂	-48*
18.05	Biphenyl	83.2	C ₁₂ H ₁₀	-1	26.66	3-Methylphenanthrene	84	C ₁₅ H ₁₂	1	32.37	Bis(2-ethylhexyl) isophthalate	84.7	C ₂₄ H ₃₈ O ₄	-35
18.18	Benzeneacetamide	84.3	C ₈ H ₉ NO	-13	27.00	2-Methylanthracene	88.5	C ₁₅ H ₁₂	-27	33.24	Decachlorobiphenyl	94.3	C ₁₂ Cl ₁₀	-81
19.27	Dimethyl phthalate	75.1	C ₁₀ H ₁₀ O ₄	8										

Table 3. Additional contaminants identified in drinking water using Pesticide PCDL for GC/Q-TOF.

RT	Compound Name	Match Score	Formula
6.17	2-Picoline	96.7	C ₆ H ₇ N
6.90	Methanesulfonate-methyl	79.6	C ₆ H ₆ O ₃ S
8.17	PPD/p-Phenylenediamine	80.0	C ₆ H ₈ N ₂
8.40	o-Toluidine	82.3	C ₇ H ₉ N
8.93	Thanite	83.9	C ₁₃ H ₁₉ N ₂ O ₂ S
9.17	Benzaldehyde	98.5	C ₇ H ₆ O
9.52	Phenol	89.6	C ₆ H ₆ O
11.46	Acetophenone	94.3	C ₈ H ₈ O
11.99	2,4,5-Trimethylaniline	82.7	C ₉ H ₁₃ N
12.90	2-Nitrophenol	77.1	C ₆ H ₅ NO ₃
22.29	DPA/Diphenylamine (DFA)	84.7	C ₁₂ H ₁₁ N
22.44	Isoxadifen	93.3	C ₁₆ H ₁₃ NO ₃
24.64	Benzylbenzoate	83.0	C ₁₄ H ₁₂ O ₂
25.96	DIBP/Diisobutyl phthalate	86.1	C ₁₆ H ₂₂ O ₄
27.00	1-Methylphenanthrene	85.3	C ₁₅ H ₁₂

Statistical analysis was performed in the MPP where the differences between Weaverville and Irvine water sources (n = 5 for each group) have been evaluated (Figure 6).

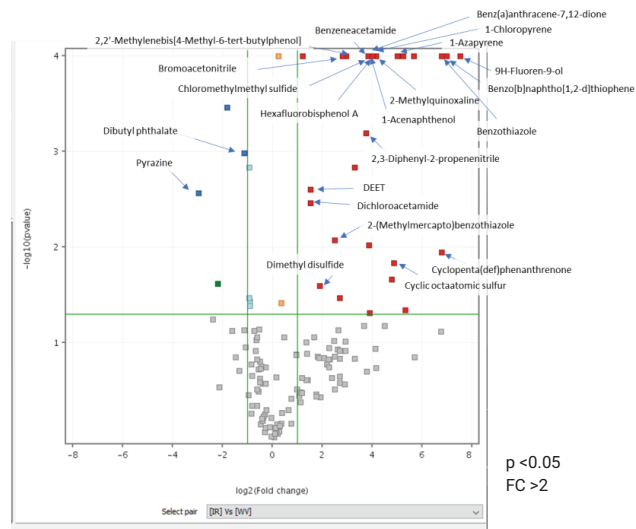


Figure 6. Comparison of water sourced in Irvine versus Weaverville using Volcano plot, showing \log_2 of Fold Change (FC) versus $-\log_{10}$ of p-Value (p). Compounds on the right part of the plot (red squares) present at higher concentrations in Irvine water extracts, those on the left (blue squares) are present at higher concentrations in Weaverville extracts.

Additionally, contaminants with high response have been reprocessed using targeted approach, and the results are shown in Figure 7.

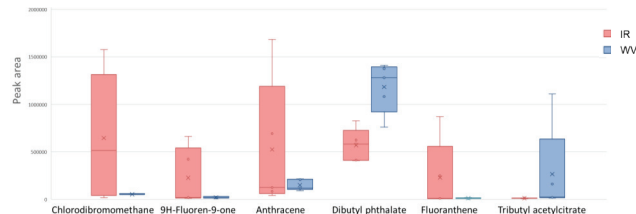


Figure 7. High abundance contaminants identified in drinking water (n = 5 for each group). IR: Irvine; WV: Weaverville.

Conclusion

- PFAS accurate mass library containing over 100 EI spectra has been created for high resolution GC/Q-TOF including several emerging volatile PFAS.
- PFAS compounds have been identified in soil and water extracts using PFAS PCDL.
- Additional contaminants have been identified in drinking water from two different source categories and included disinfection byproducts, chemicals from personal care products, drugs, pesticides and other industrial contaminants without reinjecting the sample.

Differences in Metabolic Profiles of Individuals with Heart Failure Using High Resolution GC/Q-TOF

Authors: Sofia Nieto¹, Luis Valdiviez², Oliver Fiehn², and Kai Chen¹

¹ Agilent Technologies, Inc.

² West Coast Metabolomics Center, University of California, Davis, CA

Introduction

Heart failure (HF) is a clinical condition that significantly affects the quality and duration of life of the individuals and is a major global public health problem affecting 23 million people worldwide.¹ Approximately a half of HF cases are with reduced left ventricular ejection fraction (HFrEF) while another half is characterized by preserved ejection fraction (HFpEF).² Both pathologies have similar morbidity and mortality, however, no effective treatment exists for HFpEF.² In this study, accurate mass GC/MS was used to perform metabolic profiling of individuals with both HFrEF and HFpEF to identify underlying mechanisms of this pathology that could be helpful for designing an effective treatment.

Experimental

Blood plasma was collected from subjects from HFrEF and HFpEF groups as well as healthy individuals (10 samples per each group). 30 μ L of each blood plasma sample were extracted using 1 mL of acetonitrile:isopropanol:water (3:3:2). 450 μ L of extract were dried, derivatized by O-methoximation followed by trimethylsilylation with MSTFA + 1 % TMCS. GC/MS analysis was performed using the 8890 GC coupled to the 7250 Q-TOF (Figure 1). The GC method was retention time locked to d27 myristic acid. Further details of the data acquisition method are shown in Table 1.



Figure 1. Agilent 7250 GC/Q-TOF

Table 1. GC/Q-TOF acquisition parameters

Parameter	Value
Q-TOF	Agilent 7250
GC	Agilent 8890
Column	Agilent DB-5ms UI, 30 m × 0.25 mm, 0.25 µm, DuraGuard, 10 m
Inlet	SSL, 4 mm UI liner single taper
Injection Volume	0.2 µL
Injection Mode	Splitless
Inlet Temperature	280 °C
Oven Temperature Program	50 °C for 0.5 min; 10 °C/min to 325 °C, 10 min hold
Carrier Gas	Helium
Column Flow	1 mL/min
Transfer Line Temperature	280 °C
Quadrupole Temperature	150 °C
Source Temperature	200 °C
Electron Energy	70 eV
Emission Current	5 µA
Spectral Acquisition Rate	5 Hz
Mass Range	50 to 1,200 <i>m/z</i>

The chromatographic deconvolution and library search were performed in the MassHunter Unknowns Analysis 11.1. The accurate mass Metabolomics Personal Compound Database and Library (PCDL), unit mass Fiehn Metabolomics library as well as NIST 20 were used to perform initial compound identification. Retention Indices of all three libraries were used to confirm the compound ID. Statistical analysis was performed in Mass Profiler Professional (MPP) 15.1. Structure elucidation was performed using the Molecular Structure Correlator (MSC) 8.2.

Results and discussion

Metabolic profiling

To identify metabolites involved in HFrEF and HFpEF pathophysiology, we have performed an untargeted metabolic plasma profiling of HF subjects as well as healthy individuals using a high-resolution GC/Q-TOF. The chromatographic deconvolution was performed using a highly sensitive and efficient SureMass algorithm

based on profile data, specifically optimized for complex high resolution EI spectra. Following the deconvolution and library search in Unknowns Analysis (Figure 2), the components identified in method blanks were automatically subtracted from plasma samples. Accurate mass information as well as both FAMES and Kovats retention indices (RIs) were used to confirm compound identification. The results were exported as .CEF files for further processing in MPP.



Figure 2. Deconvolution and library search results in Unknowns Analysis using (A) accurate mass metabolomics PCDL; (B) NIST 20 library. ExactMass tool (shown in outlined in red rectangles) helped to eliminate false positives based on accurate mass; this is particularly important when using unit mass libraries such as NIST. Compound ions in mirror plot are highlighted when *m/z* corresponds to the library hit formula.

Differential analysis

Statistical analysis was performed in the MPP where the differences between the HF subjects and the healthy controls have been evaluated.

To compare metabolic profiles of HF subjects and healthy individuals, the samples from the subjects of two HF pathologies have been grouped together and formed a distinct cluster from the controls (healthy individuals) as can be seen on the Principal Component Analysis (PCA) plot (Figure 3).

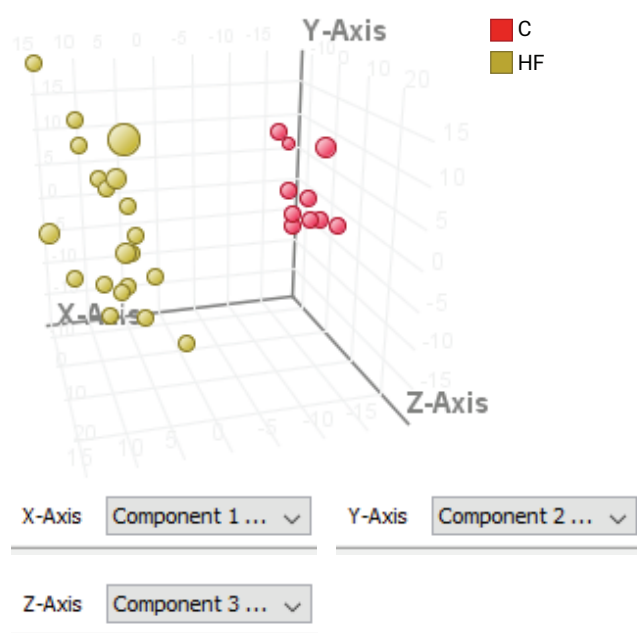


Figure 3. PCA plot showed a clear separation between the clusters of plasma samples from HF and healthy individuals (C).

Striking differences between metabolic profiles of the HF subjects as compared to the healthy individuals have been observed when using the Fold Change Analysis and visualized on a Volcano plot (Figure 4). Notably, the identified metabolites present at higher concentrations in the control samples were predominantly amino acids, while among metabolites identified at higher concentrations in plasma of HF subjects were organic acids, a few sterols and N-containing compounds, some of which could possibly be metabolites of imidazole-based drugs.

Much smaller differences were observed between the HFrEF and HFpEF groups. One of the metabolites with higher plasma levels in some of HFpEF subjects was identified as iminodiacetic acid.

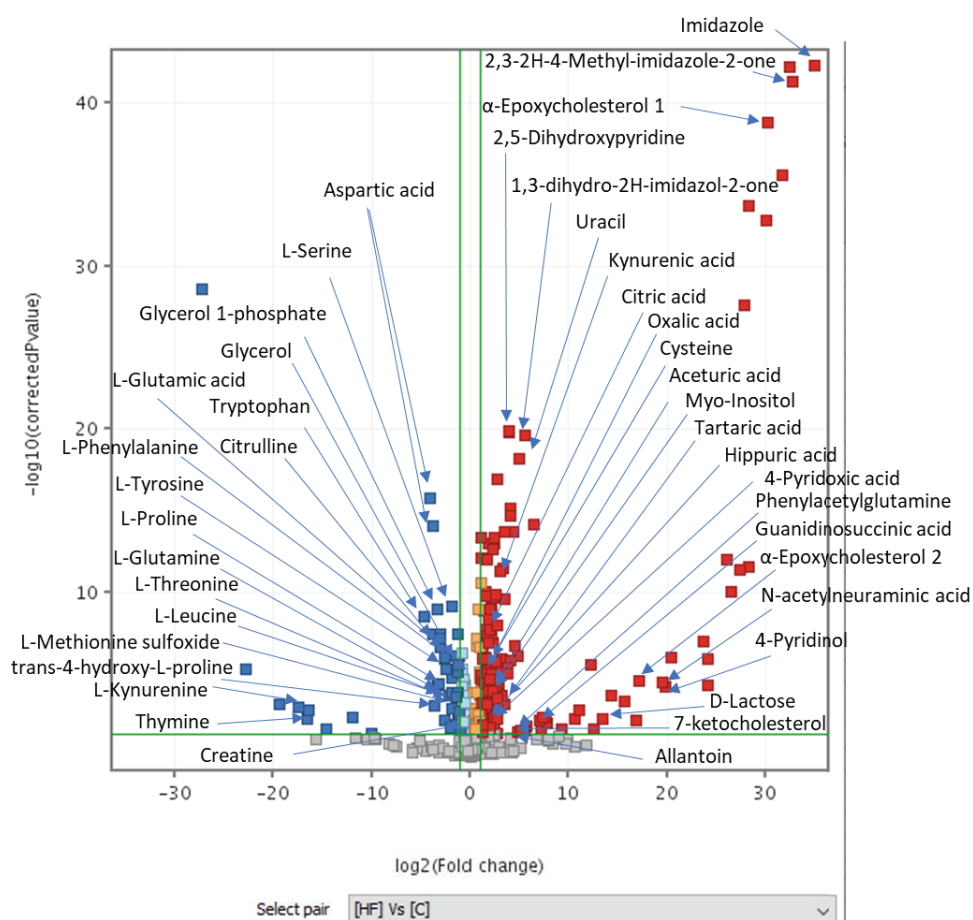


Figure 4. Volcano plot showing log of fold change (cut-off 2) versus log of p-value (cut-off 0.05) for HF subjects versus healthy individuals.

Identification of the unknown metabolites

Structure elucidation was performed for one of the unknown metabolites that was present at higher levels in the plasma of HF individuals as compared to the healthy controls. Positive CI using methane (at 20%) as a reagent gas helped to identify the molecular ion of the unknown based on the presence of $[M+H]^+$ and $[M+C_2H_5]^+$ adducts (Figure 5A).

Further, MS/MS was performed in EI at CE = 20V using the molecular ion as a precursor (Figure 5B).

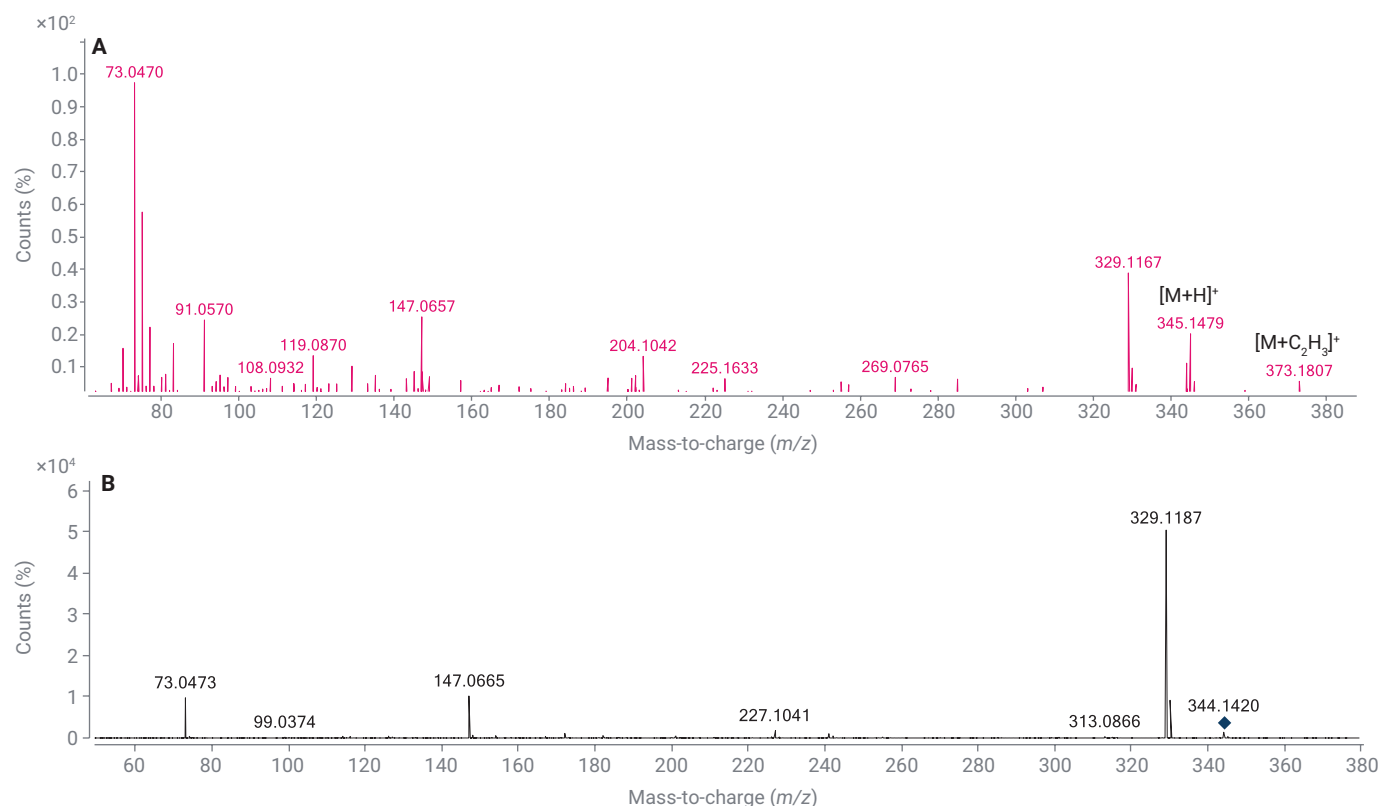


Figure 5. Positive CI (A) and EI MS/MS (B) spectra of the unknown metabolite detected in plasma of HF subjects.

Subsequent structure elucidation of the unknown was performed in MSC software using ChemSpider database as a source of the molecular structures (Figure 6). One of the top ranked structures came up as pyrimidine-2,4,6-triol.

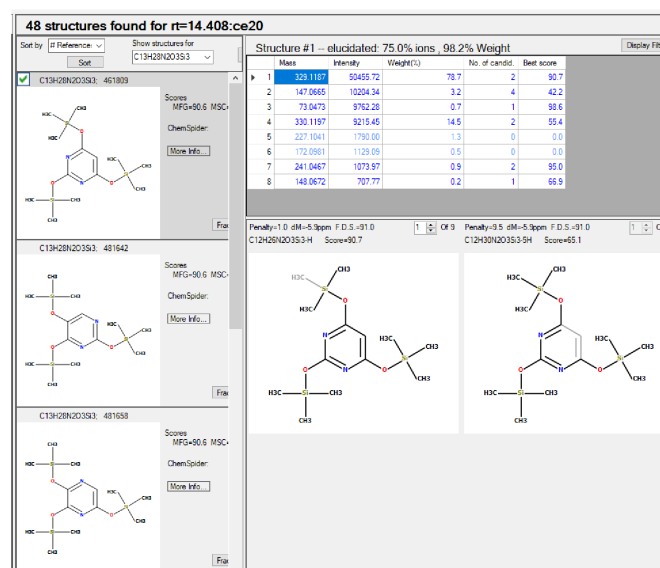


Figure 6. Structure elucidation of the unknown in MSC based on MS/MS data using the molecular ion as a precursor.

Conclusion

- Metabolic profiling of heart failure individuals has been conducted using a high-resolution GC/Q-TOF
- Over 40 metabolites have been identified as responsible for the differences between HF and healthy individuals including amino acids, organic acids and sterols
- Iminodiacetic acid was detected at higher levels in some HFpEF as compared to HFrEF individuals

References

1. Funk, M. Epidemiology of Heart Failure. *Crit. Care Nurs. Clin. North Am.* **1993** Dec, 5(4), 569–73.
2. Borlaug, B. A.; Paulus, W. J. Heart Failure with Preserved Ejection Fraction: Pathophysiology, Diagnosis, and Treatment. *Eur. Heart J.* **2011** Mar, 32(6), 670–679.

Learn more:

[**www.agilent.com/chem/gc-ms**](http://www.agilent.com/chem/gc-ms)

Find a local Agilent customer center
in your country:

[**www.agilent.com/chem/contactus**](http://www.agilent.com/chem/contactus)

U.S. and Canada

1-800-227-9770

[**agilent_inquiries@agilent.com**](mailto:agilent_inquiries@agilent.com)

Europe

[**info_agilent@agilent.com**](mailto:info_agilent@agilent.com)

Asia Pacific

[**inquiry_lsca@agilent.com**](mailto:inquiry_lsca@agilent.com)

DE65511838

This information is subject to change without notice.

© Agilent Technologies, Inc. 2023
Published in the USA, October 20, 2023
5994-6664EN

